

CASE FILE N 62 70071  
COPY

NASA MEMO 12-3-58L

11-05  
284 571

# NASA

## MEMORANDUM

AN ANALYSIS OF FLIGHT-TEST MEASUREMENTS OF THE WING  
STRUCTURAL DEFORMATIONS IN ROUGH AIR OF A  
LARGE FLEXIBLE SWEPT-WING AIRPLANE

By Harold N. Murrow

Langley Research Center  
Langley Field, Va.

NATIONAL AERONAUTICS AND  
SPACE ADMINISTRATION  
WASHINGTON  
January 1959

U

NATIONAL AERONAUTICS AND SPACE ADMINISTRATION

MEMORANDUM 12-3-58L

AN ANALYSIS OF FLIGHT-TEST MEASUREMENTS OF THE WING  
STRUCTURAL DEFORMATIONS IN ROUGH AIR OF A  
LARGE FLEXIBLE SWEPT-WING AIRPLANE

By Harold N. Murrow

SUMMARY

An analysis is made of wing deflection and streamwise twist measurements in rough-air flight of a large flexible swept-wing bomber. Random-process techniques are employed in analyzing the data in order to describe the magnitude and characteristics of the wing deflection and twist responses to rough air. Power spectra and frequency-response functions for the wing deflection and twist responses at several spanwise stations are presented. The frequency-response functions describe direct and absolute response characteristics to turbulence and provide a convenient basis for assessing analytic calculation techniques. The wing deformations in rough air are compared with the expected deformations for quasi-static loadings of the same magnitude, and the amplifications are determined. The results obtained indicate that generally the deflections are amplified by a small amount, while the streamwise twists are amplified by factors of the order of 2.0. The magnitudes of both the deflection velocities and the twist angles are shown to have significant effects on the local angles of attack at the various stations and provide the main source of aerodynamic loading, particularly at frequencies in the vicinity of the first wing-vibration mode.

INTRODUCTION

A flight investigation was recently undertaken by the National Aeronautics and Space Administration to determine the aeroelastic behavior of a large swept-wing airplane in rough air and the importance of the many factors involved in the response to gusts. Some results which are concerned with establishing the overall effects of flexibility on the wing structural strains for the test airplane in rough air are presented in references 1 and 2. These results were subsequently extended in reference 3 where the power spectra and the frequency-response functions for the measured strain responses to vertical gusts were determined. In reference 3, a comparison is made of the rough-air strain spectra

and frequency-response functions with those for a reference condition in which dynamic flexibility effects are considered negligible. From this comparison, a detailed picture at the various frequencies of the strain amplification due to dynamic flexibility was obtained.

In addition to the measurements of the wing strains, measurements were also taken of the structural deflections of the wing during the flights in rough air. The deflections are of considerable interest in problems concerning the loadings of flexible wings in rough air since they provide a direct and absolute measure of structural flexibility. Also, inasmuch as calculations for the stresses developed in the structure generally first require accurate estimates of the wing deflection response, wing-deflection data provide a convenient basis for an early evaluation of the adequacy of such calculations.

In the present paper, the wing-deflection measurements obtained from the flight tests are analyzed to determine the characteristics of the deflection and the twisting amplitudes in rough air. The form of the analysis is similar to that followed in reference 3 and involves the determination of the power spectra of the measurements and the frequency-response functions of the wing deflections and twists to vertical-gust inputs. These measured values are compared with the estimated deflections and twists for a reference condition in much the same manner as was followed for the data in reference 3. The deformation frequency-response functions, together with those of other airplane motions and the gust angle-of-attack changes, are also used to estimate the effects of the wing deformations in rough air on the local angles of attack.

#### SYMBOLS

$a_n$	normal acceleration at center of gravity, $\text{ft/sec}^2$
$c(f)$	co-power spectrum
E	modulus of elasticity, $\text{lb/sq in.}$
f	frequency, cps
G	modulus of rigidity, $\text{lb/sq in.}$
g	acceleration due to gravity, $32.2 \text{ ft/sec}^2$
h	wing deflection velocity, $\text{ft/sec}$

I	section moment of inertia, in. <sup>4</sup>
i	imaginary component of complex number
J	polar moment of inertia, in. <sup>4</sup>
$H_x^y(f)$	frequency-response function for response in $y$ to disturbance in $x$
$l_x$	streamwise distance between optigraph targets at a spanwise station, in.
$q(f)$	quadrature spectrum
t	time, sec
V	airspeed, ft/sec
$w_a$	airplane vertical velocity, ft/sec
$w_g$	vertical-gust velocity, ft/sec
$\Delta\alpha$	increment in wing local angle of attack, radians
$\gamma^2(f)$	coherency function
$\delta$	output quantity
$\theta$	pitch angle, radians
$\sigma$	root-mean-square deviation
$\Phi(f)$	power-spectral-density function
$\Psi$	phase angle by which response lags gust input, deg
$\Psi$	wing streamwise twist, radians
	designates amplitude of a complex quantity

Superscript:

- derivative with respect to time

## Subscripts:

$\bar{a}_n$	average airplane acceleration
e	reading error
F	dynamic or flexible airplane condition
h	wing deflection
R	reference airplane condition
x	arbitrary input disturbance
y	arbitrary response.

## AIRPLANE, INSTRUMENTATION, AND TESTS

The airplane used in the investigation is shown in figure 1. The configuration of the standard airplane was changed slightly for the tests by the addition of an airspeed measuring boom, a fairing on the nose, and an external canopy mounted on top of the fuselage to house the deflection recording instruments (optigraph system). Pertinent airplane characteristics are given in table I. The estimated wing-weight and fuselage-weight distributions for the rough-air tests are shown in figures 2(a) and 2(b). It should be noted that the wing stations in figure 2 are measured along the elastic axis, whereas all later figures give stations measured perpendicular to the airplane center line. All fuel weight is carried in tanks located within the fuselage as shown in figure 2(b). Figure 2(c) presents the calculated wing-bending-stiffness (EI) distribution and the experimental torsional-stiffness (GJ) distribution for the wing.

The optigraph system used herein consisted of a camera which was located on top of the fuselage for recording the deflections of six target lamps on the left wing. (The target lamps were located near the front and rear spars as shown in fig. 3.) High-intensity infrared light sources were used in combination with infrared-sensitive recording film. A more detailed description of the optigraph system and some results obtained from using this system for the airplane in maneuvers are given in references 4 and 5. (Note that the targets of concern herein are numbered 9 to 14 to agree with the notation used in ref. 4.) The sensitivity factors are given in table II. The instrument response is invariant with frequency because of the direct-type measurements obtained from the optigraph system.

In addition to the deflection recordings, the following records were used to determine the gust input both for a definition of the turbulence and for use in frequency-response determinations:

- (1) Normal acceleration at center of gravity
- (2) Pitch velocity
- (3) Pitch angle (obtained by integrating the pitch-velocity record)
- (4) Airspeed
- (5) Vane angle of attack

Other records used in the data evaluations were control-position records, which provided a check that control movements were not large or abrupt during the gust runs, and motion-picture-camera recordings of the fuel gages for use in determining the airplane weight. The film speed of the individual recorders was  $1/4$  in./sec, with the exception of the optigraph equipment which recorded at a film speed of 3 in./sec for better time resolution. An NACA  $\frac{1}{10}$ -second chronometric timer was used to synchronize all the records.

The rough-air data presented herein are from a 90-second test run in clear-air turbulence at a Mach number of 0.58 and a pressure altitude of 5,500 feet (approximately 3,000 feet above the terrain). The airplane weight was 117,200 pounds, and the center-of-gravity position was at 20.2 percent of the mean aerodynamic chord. The piloting procedure was essentially "stick free," and any required corrections deemed necessary by the pilot were effected by small and gradual control movements.

In addition to the rough-air tests, a series of slow pull-up maneuvers in smooth air were also made at various combinations of Mach number, weight, and altitude in order to obtain the variation of deflection per  $g$  and twist per  $g$  with dynamic pressure. These so-called pull-up factors are used in connection with the reference condition which will be described later.

#### METHOD

The basic method used in the present investigation is essentially the same as that of reference 3. The measurements of wing deflections and twists (twist is the difference between front- and rear-spar deflections, divided by the streamwise distance between them), along with the measurements of the turbulence encountered during the flight tests,

provided the basic data for determining the deflection and twist response characteristics of the airplane.

For comparison with the rough-air measurements, reference values of the responses are obtained for equivalent static-type loadings. The determination of these reference values involves the use of (1) faired center-of-gravity acceleration measurements which approximate the airplane loading in rough air, and (2) data from slow pull-up maneuvers which provide values of deflection and twist per unit airplane loading in quasi-static load applications.

Since the various records used in the analysis exhibited irregular and random-type time histories, techniques of random-process theory were used as in reference 3 for an adequate description of the response characteristics. In this connection, power spectra and cross-spectra are used. The detailed procedures followed in the data analysis are described in subsequent sections of this report.

#### EVALUATION OF DATA AND RESULTS

The evaluation of the data involved the following steps:

- (1) Evaluation of the pertinent time-history recordings (These included the wing deflection and twist measurements from the optigraph records, the normal acceleration recorded at the center of gravity, and the angle-of-attack indications and the records of the associated airplane motions used to obtain vertical-gust velocity.)
- (2) Evaluation of the deformation and acceleration records taken during slow pull-up maneuvers to establish the reference quasi-static condition
- (3) Evaluation of the necessary power spectra and cross-spectra
- (4) Determination of the frequency-response functions for the deflection and twist responses to vertical gusts
- (5) Estimation of the effects of the structural deformations of the wing in rough air on the changes in local angle of attack

The procedures used in these evaluations are described in the following paragraphs.

### Time-History Measurements

Sample sections of the evaluated time histories of the wing bending and twist measurements at the various stations, the center-of-gravity acceleration, and the vertical-gust velocity are given in figure 4 to illustrate the general characteristics of the records obtained in rough air. The four parts of figure 4 permit comparisons to be made in the following order:

- (1) Front- and rear-spar deflections at the various stations (fig. 4(a))
- (2) Rear-spar deflections for the various stations, vertical-gust velocity, and acceleration at the center of gravity (fig. 4(b)). (Note that the faired center-of-gravity acceleration is also shown and is discussed subsequently.)
- (3) Twist at the three spanwise stations, vertical-gust velocity, and normal acceleration at the center of gravity (fig. 4(c))
- (4) Rear-spar deflections and twists at the various stations (fig. 4(d))

The reading interval of 0.1 second used in the time-history evaluation was selected on the basis of record examinations which indicated that almost all wing motions occurred at frequencies less than 5 cps.

The time histories of wing twist in figures 4(c) and 4(d) were obtained from the difference between the front- and rear-spar deflections at the separate stations, divided by the streamwise distance between target locations. In determining these twists for station 383, the rear-spar-deflection measurements at station 389 were adjusted for streamwise misalignment of the target lamps (see fig. 3) through linear interpolation.

The time history of the vertical-gust velocity was evaluated by correcting the flow-direction vane measurements for the vertical velocity and pitching motions of the airplane by the procedures described in reference 3. For this evaluation a visual fairing of the flow-vane records was made in order to remove the effects of a 7 cps oscillation which resulted from boom vibrations. As will be discussed later, this fairing may affect the reliability of the gust-velocity measurements at the higher frequencies.

### Reference Values

In order to obtain a measure of the effects of structural flexibility on the deflections and twists at the various locations, a set of reference values is desirable for comparison with the actual measured values in rough air. The method used in reference 3 for obtaining

such reference values was followed in the present case and involves the determination of values of deflection per unit airplane loading in the quasi-static (pull-up) condition and a determination of the aerodynamic loading applied to the airplane in rough air. The reference values obtained may be viewed as an approximation to the outputs that would be obtained for a quasi-static airplane; that is, an airplane restrained from dynamic vibration. This procedure essentially neglects the interaction between the dynamic airplane vibrations and the aerodynamic forces and assumes that the span-load distribution and the proportion of load carried by the wing and tail is the same in gusts as in pull-ups.

The pull-up maneuvers used in establishing the reference values were made at several altitudes and airspeeds in order to obtain a variation in dynamic pressure. As was the case for the strain indications in references 1 to 3, the relation between deflection and center-of-gravity acceleration in maneuvers was linear. The pull-up factors (deflection per g) were then plotted against dynamic pressure as shown in figure 5. The data points shown in figure 5 have incorporated in them a weight correction which was obtained from pairs of slopes at the same dynamic pressure and different weights. An extrapolation of a line through the data points gave pull-up factors for the value of dynamic pressure of the gust run. Figure 5 shows this extrapolation for pull-up factors of front- and rear-spar deflection at station 517 and is typical of the other stations. The resulting pull-up factors obtained in this manner for deflections and twists are shown in table II and are used to obtain reference deflections and twists for comparison with the rough-air data.

For the determination of the aerodynamic loading or average airplane acceleration in rough air, use was made of the record of normal acceleration at the center of gravity. As was shown in reference 1, for this airplane, the average airplane acceleration can be closely approximated if the effects of vibrations are removed by a visual fairing of the record of normal acceleration at the center of gravity. This procedure was applied in the present case and a 15-second portion of the unfaired and faired record is shown in figure 4(b).

#### Power Spectra

The procedures outlined in reference 6 were used to determine power spectra. For present purposes, estimates of the power were obtained for 61 frequency intervals equally spaced from 0 to 5 cps. For convenience, and since no appreciable power is present at higher frequencies, the spectra are shown only to 3 cps. The power spectra of the deflection measurements are shown in figure 6(a), and the twist spectra are shown in figure 6(b). In each case, the reference power spectrum is shown. From the airplane acceleration and pull-up factors, the reference spectra are obtained as follows:

$$(\Phi_\delta)_R = \Phi_{\bar{a}_n} (\delta/a_n)^2 \quad (1)$$

where

$\delta$  measured output quantity of interest (in the present case, deflection or twist)

$\bar{a}_n$  average airplane acceleration in rough air (faired record of acceleration at center of gravity)

$\delta/a_n$  pull-up factor

Note that the reference spectra are essentially the spectra of the faired center-of-gravity acceleration multiplied by a constant.

Also shown in figures 6(a) and 6(b) are values of the root-mean-square deviation of the deflection and twist records. These values are also given in table II. An estimate of the overall difference or amplification of the response of the airplane to dynamic loading above that of quasi-static loading is given by the ratio of the root-mean-square value of deflection or twist to the reference value of root-mean-square deviation. These ratios are listed in table II and are obtained as follows:

$$\frac{\sigma_F}{\sigma_R} = \frac{\sigma_\delta}{(\delta/a_n)(\sigma_{\bar{a}_n})} \quad (2)$$

In regard to the fairing of the record of center-of-gravity acceleration, it is of interest to compare the spectrum of the record of center-of-gravity acceleration with the spectrum of the record of faired center-of-gravity acceleration. These spectra are shown in figure 7. From this comparison, it can be seen that an attenuation of the power has been accomplished at the higher frequencies as was desired.

The spectrum of vertical-gust velocity is shown in figure 8. The power drops off quite rapidly with frequency and, in fact, drops off more rapidly than observed in previous gust measurements in which the power at the higher frequencies varied approximately as  $1/f^2$ . This more rapid decrease in power with frequency is probably a consequence of the fairing of the record of the vane-measured angle of attack and serves to make the measured spectrum of doubtful reliability at frequencies above 1.5 or 2 cps, as was mentioned previously.

Cross-spectra were obtained for the determination of frequency-response functions. From 0.1-second readings, cross-spectra were obtained between the gust velocity and each of the deflection and twist responses. In addition, the cross-spectrum between gust velocity and faired center-of-gravity acceleration was obtained for use in determining reference frequency-response functions. In all cases, 60 lags were used to obtain the cross-spectra correlation functions.

#### Frequency-Response Functions

The procedure used in determining the frequency-response functions is based on the relation between the spectrum of an input disturbance  $\Phi_x(f)$  and the cross-spectrum between the input disturbance and the response  $\Phi_{xy}(f)$  and is referred to as the cross-spectrum method in reference 3. The frequency-response function  $H_x^y(f)$  is given as follows:

$$H_x^y(f) = \Phi_{xy}(f)/\Phi_x(f) = \frac{c_{xy}(f) - i\alpha_{xy}(f)}{\Phi_x(f)} \quad (3)$$

where  $H_x^y(f)$  defines the system response in  $y$  to unit sinusoidal disturbances in  $x$ . From equation (3), the amplitude of  $H_x^y(f)$  is given as:

$$|H_x^y(f)| = \frac{|\Phi_{xy}(f)|}{\Phi_x(f)} \quad (4)$$

and the phase lag  $\psi$  of the output behind the input is given as:

$$\psi = \text{arc tan } \frac{q(f)}{c(f)} \quad (5)$$

By using the preceding equations, frequency-response functions were obtained between vertical-gust velocity and the output deflections and twists at the various stations. The actual numerical procedures are described in detail in references 3 and 6 and will, therefore, not be repeated herein. The amplitudes and phases of the resulting

frequency-response functions are shown by the solid curves in figure 9. Since the amplitudes and phases become quite erratic and, as will be shown later, unreliable at frequencies above 2.5 cps, values at the higher frequencies are not shown.

For comparison with the rough-air frequency-response functions, reference frequency-response functions were determined from cross-spectra between gust velocity and faired center-of-gravity acceleration. In order to convert the frequency-response function for airplane acceleration to corresponding units of deflection or twist, reference pull-up factors for each of the stations were used. Thus, the reference frequency-response function for each station is obtained as follows:

$$\left[ H_{wg}^{\delta}(f) \right]_R = \frac{\Phi_w g \bar{a}_n(f)}{\Phi_{wg}(f)} (\delta/a_n) \quad (6)$$

where the appropriate pull-up factors given in table II are used. The amplitudes and phases of the reference frequency-response functions are shown by the dashed curves of figure 9. The differences between the frequency-response functions for the dynamic and reference conditions represent the effects of structural dynamics on the deflections and twist responses at the various frequencies.

#### Effects of Structural Deformations on Local Angles of Attack

In order to obtain a measure of how the structural deformations affect aerodynamic loadings, the contributions of the wing flexible motions to the changes of the local angles of attack in rough air were examined. Changes of the local angle of attack at a given wing station in rough air may be expressed by the following equation:

$$\Delta\alpha_F(t) = \Delta\alpha_{wg}(t) + \Delta\alpha_\theta(t) + \Delta\dot{\alpha}_\theta(t) + \Delta\alpha_{wa}(t) + \Delta\alpha_h(t) + \Delta\alpha_\varphi(t) \quad (7)$$

where each term on the right designates the contribution to the angle-of-attack change arising from the gust velocity and the specified motions. A check has shown that the term due to pitching velocity  $\dot{\theta}$  is insignificant; therefore, this term will be neglected. At any time  $\Delta\alpha_F$  is then given by

$$\Delta\alpha_F = \frac{w_g}{V} + \theta + \frac{w_a}{V} - \frac{\dot{h}}{V} + \varphi \quad (8)$$

where each term is in radians. The terms on the right represent, respectively, the contributions of the vertical gust, pitch attitude, airplane vertical velocity, wing deflection velocity, and streamwise twist.

From equation (8) the frequency-response function for the local angle of attack may be expressed in terms of the associated frequency-response functions for the various motion responses to vertical gusts as follows:

$$\frac{\Delta\alpha}{w_g}(f) = \left[ H_{w_g}^{\Delta\alpha}(f) \right]_F = \frac{1}{V} H_{w_g}^{w_g}(f) + H_{w_g}^{\theta}(f) + \frac{1}{V} H_{w_g}^{w_a}(f) - \frac{1}{V} H_{w_g}^h(f) + H_{w_g}^{\Phi}(f) \quad (9)$$

where the frequency-response functions are complex quantities. The frequency-response functions for pitch and vertical motion were determined from measurements of the pitch angle and from an integration of the measurements of normal acceleration, respectively. The frequency-response functions for the deflection velocity and twist contributions to the changes of the local angles of attack are determined from results presented earlier for deflections and twist. The determination of the contribution of the flexible motions to the total angle-of-attack changes requires vectorial addition of the terms given in equation (9). As was done in earlier sections of the paper, a reference is used for comparison with the rough-air results. The reference frequency-response function is obtained as follows:

$$\frac{\Delta\alpha}{w_g}(f) = \left[ H_{w_g}^{\Delta\alpha}(f) \right]_R = \frac{1}{V} H_{w_g}^{w_g}(f) + H_{w_g}^{\theta}(f) + \frac{1}{V} H_{w_g}^{w_a}(f) + H_{w_g}^{\Phi_R}(f) \quad (10)$$

A comparison of equation (10) with equation (9) shows that with the exception of the last term in equation (10), the reference frequency-response function does not include the flexible motions. The last term includes only the quasi-static portion of streamwise twist. This term is the reference frequency-response function of figure 9(c).

Figure 10 presents a comparison of the frequency-response functions for the local angle-of-attack changes  $\left[ H_{w_g}^{\Delta\alpha}(f) \right]_F$  with the reference frequency-response function  $\left[ H_{w_g}^{\Delta\alpha}(f) \right]_R$  and shows the variation with

frequency of both  $\frac{\Delta\alpha_F}{w_g}(f)$  and  $\frac{\Delta\alpha_R}{w_g}(f)$  at the three stations. Inspec-

tion of the curves shows that at the very low frequencies the angle-of-attack changes due to the gust velocity are alleviated somewhat by both the dynamic and reference airplanes. At the higher frequencies the gust effects are amplified by the motions, particularly near the frequency of the fundamental wing bending mode. The difference between the two curves in figure 10 represents the net contributions of the flexible motions to the angle-of-attack changes at the three stations. This difference shows that the flexible motions act in the direction to alleviate the gust-induced angle-of-attack changes up to frequencies of about 1 cps; above this the flexible motions act to increase or amplify gust-induced angle-of-attack changes by large amounts.

#### GENERAL REMARKS ON RELIABILITY OF RESULTS

A fairly detailed consideration of the reliability of the present estimates of the frequency-response functions is given in the appendix. Some general remarks concerning the results in the appendix appear warranted here. The present estimates of the frequency-response functions have two principal types of error. The first is a purely statistical or sampling error arising from the limited length of the record. The magnitude of the statistical errors are defined by the confidence bands of figure 11. These confidence bands indicate that the statistical reliability of the amplitudes is roughly  $\pm 30$  percent to frequencies slightly above 1 cps and of the phase angles is  $\pm 20^\circ$  between 0.3 and 1.5 cps. The second type of error is a systematic error or distortion arising from the presence of extraneous noises. As indicated in the appendix, a number of such noise sources are present and their effects cannot be precisely estimated. Generally, it appears that the present estimates may be too low due to these errors.

The usable results are within 0.3 to 1.8 cps; outside this frequency range, the errors become larger and more difficult to evaluate.

#### DISCUSSION

##### Power Spectra

Examination of figure 6(a) indicates that the power spectra of wing deflections are quite similar at the various locations. In each case, the largest peak is at the short-period frequency of about 0.5 cps

and a secondary peak is present at the frequency of the fundamental wing bending mode of 1.5 cps. Subsidiary power peaks are also evident and are associated with higher structural modes. As noted in reference 7, the small peak at 2.1 cps is caused by an antisymmetric mode at that frequency. The power peaks and the total power of the deflection measurements increase progressively for the successive outboard stations. The root-mean-square deflection values for the front-spar measurements increase in the outboard direction and vary from about 1.0 to about 3.4. For the rear-spar deflection measurements, the root-mean-square values are slightly higher.

Comparison of the measured deflection power spectra (dynamic) with the reference spectra in figure 6(a) indicates that at the lower frequencies (up to about 0.75 cps), the power in rough air is lower than that of the reference, while at the higher frequencies, the measured power spectra of the deflections show considerable amplification above what the deflections would have been if the load were applied quasi-statically. The undershoot at the lower frequencies is somewhat surprising and is not clearly understood; it may be a consequence of coupling effects between the short-period mode and the first bending mode. The effects of the structural dynamics on the root-mean-square deflection magnitudes may be seen from the ratios of measured root-mean-square values at each station to the reference root-mean-square values  $\left( \frac{\sigma_F}{\sigma_R} \right)$ . These ratios listed in table II show that the wing deflec-

tions are amplified by an overall amount of about 5 to 10 percent due to flexibility. Considering this result and from observations of the spectra, it is seen that the fairly large amplifications at higher frequencies are nearly compensated by the reductions at lower frequencies.

The power spectra of wing twist shown in figure 6(b) have distinctive differences from the deflection spectra. The main power peak of the twist power spectra is at the frequency of the fundamental wing bending mode. The power peak at the short-period mode is less prominent and a smaller peak is evident at 2.1 cps. The amplitude of the power peaks and the total twist power increase in the outboard direction, as was the case for the deflection spectra. Root-mean-square twist values increase from about 0.002 radian at the inboard station to about 0.007 radian at the outboard station.

Comparison of the measured power spectra of twist with the reference power spectra indicates that the dynamic amplifications in the twist motions are considerably larger than was the case for the deflections. Relative to the reference condition, the ratios of root-mean-square twist values, as shown in table II, increase from about 1.6 at the inboard station to about 2.7 at the outboard station. Some of the difference between deflection and twist ratios may be attributed to

reading errors since these are larger proportionally for twist than for the deflection measurements and increase the total area under the twist spectra by about 20 percent. Since this is only a part of the differences in amplification between deflections and twist, however, the twist amplification is still significantly greater than that of the deflection response.

### Frequency-Response Functions

The frequency-response functions of figure 9 represent particularly useful results of the present study in that they serve to define the deformation characteristics of the test airplane independent of the input in terms of actual measured values of deflection and twist amplitudes for the present set of flight conditions. These frequency-response functions are thus suitable for direct comparisons with analytic calculations. A comparison of the curves of figure 9 shows that, for both deflections and twists, the flexible airplane (solid curve) has much greater response than the reference airplane (dashed curve) at frequencies of 1.5 and 2.1 cps. While the twists for the dynamic (flexible) condition are nearly always greater than those for the reference condition throughout the complete frequency range, the deflections for the dynamic condition are consistently less than those for the reference condition up to frequencies of 0.75 cps. This same result was noted upon inspection of the spectra. The phase angles show an increasing lag with frequency of the measured values with respect to those for the reference condition.

### Effects of Deformations on Local Angles of Attack

The amplitudes and phases of the frequency-response functions of deflections and twists were used to obtain estimates of their effects on local angles of attack. These results are shown in figure 10 where values of  $\Delta\alpha/w_g$  less than 1 show that the contributions of the flexible motions to the incremental angle of attack tend to alleviate the gust-induced angle of attack and values of  $\Delta\alpha/w_g$  greater than 1 indicate that flexible motions tend to amplify the gust-induced angle of attack. It is evident from the solid curve that at the very low frequencies the direct gust-induced angle-of-attack increment and associated load are alleviated somewhat, while at the higher frequencies, particularly at the frequency of the fundamental wing bending mode, local angles of attack are greatly amplified by the deformations. The effects of the rigid body and quasi-static twist motions of the reference airplane on the local angles of attack are also indicated in the figure (dashed curve) and show that these motions tend to amplify the gust-induced angle of attack at frequencies of 0.25 to 1.35 cps. By comparing the two curves, it is evident that the local angles of attack due to motions of the reference

airplane are alleviated by the flexible motions up to frequencies of about 1.0 cps. Above 1.0 cps, flexibility amplifies the local angle of attack with the greatest amount of gust amplification occurring at about 1.6 cps. At this frequency, the twist and bending velocity increase the gust-induced angle of attack by factors between 2 and 3.

#### CONCLUDING REMARKS

The foregoing analysis has served to define the characteristics of the wing deflection and twisting amplitudes of a large flexible airplane in rough air. For the test conditions, the power spectra of the wing deflections contain two prominent peaks: one at 0.5 cps associated with the short-period mode, and the other at about 1.5 cps associated with the first wing bending mode. Comparison of the power spectra of deflections in rough air with the quasi-static reference power spectra of deflections indicates that at frequencies above about 1 cps the effects of flexibility induce large dynamic amplifications of the deflections, while at low frequencies an attenuation is evident. The overall wing deflections, as measured by ratios of root-mean-square values, are generally amplified about 5 to 10 percent in rough air.

The twist spectra exhibit peaks at about the same frequencies as the deflection spectra; however, the principal peak of the twist spectra is at the frequency of the fundamental wing bending mode. The spectra of twist measured in rough air is higher throughout the frequency range than the twist spectra for the reference condition. The ratios of root-mean-square streamwise twists (dynamic to quasi-static reference) are much larger than those for deflection measurements, and the ratios vary from about 1.5 to 2.8.

Frequency-response functions were determined for the airplane deflection and twist responses to vertical gusts. These are particularly useful for comparison with analytical calculations. The frequency range from 0.3 to 1.8 cps appears to be the reliable range of the results. The overall results show that both the deflection and twist responses per unit gust velocity are greatest near the frequency of the fundamental wing bending mode. The twist responses relative to the reference responses appear to be much larger than those of the deflections.

An analysis of the effects of the wing deflections and twists on the wing local angles of attack indicates that the flexibility acts to reduce the angles of attack at frequencies below about 1.0 cps and to increase the angles of attack by large amounts in the region of the fundamental wing vibration mode at 1.5 cps.

Langley Research Center,  
National Aeronautics and Space Administration,  
Langley Field, Va., October 1, 1958.

## APPENDIX

## RELIABILITY OF RESULTS

The general problem of determining the reliability of frequency-response-function estimates for rough-air flight tests was considered in detail in reference 3. Results of general applicability were derived therein and are applied to the evaluation of the reliability of the frequency-response functions for the strain responses for the present airplane to rough air. The same considerations will, for the most part, apply to the present problem, and the discussion will be based accordingly on the results given in reference 3.

The basic sources of error in the present estimates of the frequency-response functions arise from:

- (1) Basic accuracy of the deflection, twist, and gust-velocity measurements
- (2) The effects of extraneous factors (factors other than the vertical-gust velocity) on the deflection and twist results (These include other components of turbulence, spanwise variations in turbulence, and pilot-control motions.)
- (3) Statistical or sampling errors resulting from the finite record length.

The manner in which each of these error sources affects the present results will be considered subsequently.

## Deflection and Twist Measurements

The optigraph system (measuring deflections) has a fairly high degree of accuracy. A loss of accuracy in the measured values does, however, arise from record sensitivity, record-trace thickness, and the manual reading of the records. Checks have indicated that the present record-reading procedure yields random-type reading errors with a relatively flat power spectrum and with  $\sigma = 0.002$  inch of film deflection. (This value of root-mean-square reading error is less than 0.003, the value usually quoted for readings of this type, and was estimated from repeated readings of the records. The high film speed used was also helpful in that the slope of the record trace was low at all times.) With the sensitivity factors for the present records of a 35-inch to 48-inch wing deflection per inch of film deflection, the root-mean-square reading error of 0.002 gives a root-mean-square wing-deflection

error of 0.07 to 0.10 inch. These values of  $\sigma_e$  given in table II are a small part (about 3 to 8 percent) of the measured root-mean-square deflections and do not affect significantly the measured root-mean-square values. However, they do affect the reliability of the power spectra at frequencies where the signal power is low. In the present case, a rapid decrease in the power spectrum with frequency occurs above 1.5 cps. At these frequencies, the reading-error power is large relative to the actual deflection power, particularly at station 383 where the deflections were lowest. As indicated in reference 3, reading errors in the output yield additive errors to the power spectrum. Thus, the power spectra may be expected to be too high, particularly in regions of low power. The cross-spectrum between the gust and the deflection and the estimated frequency-response functions are, however, largely unaffected by these errors.

The twist measurements (obtained from the difference of two deflections) have a reading error which is much larger relative to measured values than was the case for the deflections. As indicated by the values in table II, the ratio of root-mean-square reading error to root-mean-square twist value is 0.44 at the inboard station and decreases to about 0.25 at the outboard station. For the twist case, then, the root-mean-square values are significantly increased by the reading errors. In addition, the distortion of the power spectra of the twist may be expected to be large at regions of low power. However, frequency-response functions obtained using cross-spectra should not be greatly affected by reading errors in the twist measurements.

#### Gust-Velocity Measurements

The reliability of the gust spectrum is affected by a large number of factors. Dominating factors at the higher frequencies (above about 2.5 cps) are vane sensitivity and reading errors, and at the low frequencies (below about 0.3 cps), the dominating factor is the reliability of the measured pitch attitude. In addition, the fairing of the high-frequency oscillations from the vane record affects higher frequencies and possibly extends to frequencies as low as 2 cps. While the reading errors tend to overestimate the input power, the record fairing contributes to an underestimation of the power. While no precise value can be given for the total effective distortions of the gust spectrum, it is probable that the distortions in the frequency range from 0.3 to 2 cps are in the direction to cause the amplitudes of the frequency-response functions to be too low by approximately 20 percent. Below about 0.3 cps and above 2 cps, the distortions are significantly larger and difficult to evaluate. As a consequence, the frequency-response-function estimates are not considered reliable in these frequency regions.

### Extraneous Factors

Prominent among the factors influencing the frequency-response function, other than the vertical-gust velocity, are spanwise variations in gust velocity, other components of turbulence, and pilot-control motions. The effects of these factors are similar in nature and magnitude to those that were considered to apply to the strain results in reference 3. The spanwise effects result in a small underestimation of the amplitude of the frequency-response functions at low frequencies, and this underestimation increases to about 10 to 15 percent at 2 cps. Other components of turbulence and pilot-control motions are considered to affect the present results, principally at very low frequencies (below 0.3 cps). These factors may contribute to the reduction in coherency at these low frequencies and also introduce distortions to overestimate the magnitude of the frequency-response function.

### Coherency Functions

As indicated in reference 3, the concept of a coherency function is a prime factor in reliability considerations. The coherency function is defined as

$$\gamma^2(f) = \frac{|\Phi_{xy}(f)|^2}{\Phi_x(f) \Phi_y(f)} \quad (11)$$

where

$\Phi_x(f)$  power spectrum of input disturbance or, in the present case, vertical-gust velocity

$\Phi_y(f)$  power spectrum of response of interest (primarily deflections and twists)

$\Phi_{xy}(f)$  cross-spectrum between input disturbance and response

The value of the coherency function determines the size of the statistical or sampling errors and also provides an indication of the possible presence of distortions in the results. For a perfect input-output system, the coherency function is equal to 1. On the other hand, if the measured input and output are entirely unrelated, the coherency function is equal to 0. In any given case, the actual values of the coherency function will lie between 0 and 1, and the amount of reduction from a value of 1 provides an indication of the degree to which disturbing or extraneous elements are present.

Values of the coherency function can be determined directly from the measured results by the application of equation (11). Figure 12 presents the results obtained from the present measurements for the coherency functions between the vertical-gust velocity and the measured deflections and between the vertical-gust velocity and the measured twist. For the deflection results, only the front-spar values are shown, inasmuch as the values for the rear spar were similar. An examination of the results for the deflections (fig. 12(a)) indicates

(1) Fairly high coherencies (about 0.8) for the frequency range from 0.2 to 1.0 cps

(2) Very low coherencies at frequencies below 0.2 cps and above 1.8 cps.

Also shown in figure 12(a) is the coherency function between the gust velocity and faired center-of-gravity acceleration.

For the twist measurements (fig. 12(b)), the coherencies followed the same general pattern as for the deflection measurements, except that the curves were generally slightly lower. On the basis of the results of reference 3, it would appear that reliable frequency-response functions in the present investigations can at best only be obtained for the frequency region from 0.2 to about 1.8 cps. Even for this frequency region, there exists the possibility that distortion in the estimates may be present and associated with the measured reductions in coherencies. In order to assess the magnitudes of these distortions, it will be necessary to consider the character and magnitude of the errors arising from the various sources listed previously.

#### Distortions

The foregoing discussion has indicated that a number of sources of distortion are present in the estimated frequency-response functions. The most important sources of distortion are reading errors and spanwise gust variations. In general, the magnitudes of these distortions are probably less than 20 percent between about 0.3 and 1.8 cps and cause the amplitudes of frequency-response systems to be underestimated. At frequencies below 0.3 and above 1.8 cps, the distortions are much larger and more difficult to estimate. Thus, the results in these regions are of little value.

#### Confidence Bands

The sampling errors are also significant and depend heavily on the sample length and coherency functions. Confidence bands, which for a given probability level (90 percent in the present case) provide a measure

of the range within which the true value may be expected, were obtained for the present paper according to the procedure of reference 3. (This procedure is based on the results of ref. 8.) Typical confidence bands are shown in figure 11 for both the amplitude and phase lag for a deflection and a twist frequency-response function. Examination of the figure shows that amplitudes are reliable within  $\pm 30$  percent to frequencies slightly above 1 cps; beyond this value, the reliability decreases quite rapidly. The confidence bands for the phase angles appear to be reliable within  $\pm 20^\circ$  between 0.3 and 1.5 cps and appear less reliable elsewhere.

#### Reference (Pull-Up) Values

Errors in the values obtained under steady-loading conditions affect the amplitudes of the curves for the reference condition shown in figure 9. The actual frequency-response functions measured in rough air are not affected by these values. The relation between the flexible and reference conditions is affected and the apparent amplification is modified by these differences. The static values of deflection per g (table II) are believed to be accurate within 0.20 inch per g. Accordingly, the quasi-static values of twist per g are believed accurate within 0.002 radian per g.

## REFERENCES

1. Rhyne, Richard H., and Murrow, Harold N.: Effects of Airplane Flexibility on Wing Strains in Rough Air at 5,000 Feet As Determined by Flight Tests of a Large Swept-Wing Airplane. NACA TN 4107, 1957.
2. Rhyne, Richard H.: Effects of Airplane Flexibility on Wing Strains in Rough Air at 35,000 Feet As Determined by a Flight Investigation of a Large Swept-Wing Airplane. NACA TN 4198, 1958.
3. Coleman, Thomas L., Press, Harry, and Meadows, May T.: An Evaluation of Effects of Flexibility on Wing Strains in Rough Air for a Large Swept-Wing Airplane by Means of Experimentally Determined Frequency-Response Functions With an Assessment of Random-Process Techniques Employed. NACA TN 4291, 1958.
4. Mayo, Alton P., and Ward, John F.: Flight Investigation and Analysis of the Wing Deformations of a Swept-Wing Bomber During Push-Pull Maneuvers. NACA RM L54K24a, 1955.
5. Mayo, Alton P.: Flight Investigation and Theoretical Calculations of the Fuselage Deformations of a Swept-Wing Bomber During Push-Pull Maneuvers. NACA RM L56L05, 1957.
6. Press, Harry, and Tukey, John W.: Power Spectral Methods of Analysis and Their Application to Problems in Airplane Dynamics. Vol. IV of AGARD Flight Test Manual, Pt. IVC, Enoch J. Durbin, ed., North Atlantic Treaty Organization, pp. IVC:1 - IVC:41.
7. Coleman, T. L., Murrow, H. N., and Press, Harry: Some Structural Response Characteristics of a Large Flexible Swept-Wing Airplane in Rough Air. Preprint No. 785, S.M.F. Pub. Fund Preprint, Inst. Aero. Sci., Jan. 1958.
8. Goodman, N. R.: On the Joint Estimation of the Spectra, Cospectrum and Quadrature Spectrum of a Two-Dimensional Stationary Gaussian Process. Scientific Paper No. 10 (BuShips Contract Nobs-72018 (1734-F) and David Taylor Model Basin Contract Nonr-285(17)), Eng. Statistics Lab., New York Univ., Mar. 1957.

TABLE I.- PERTINENT PHYSICAL CHARACTERISTICS AND  
DIMENSIONS OF TEST AIRPLANE

Total wing area, sq ft . . . . .	1,428
Wing span, ft . . . . .	116
Wing aspect ratio . . . . .	9.43
Wing thickness ratio . . . . .	0.12
Wing taper ratio . . . . .	0.42
Wing mean aerodynamic chord, in. . . . .	155.9
Wing sweepback (25-percent-chord line), deg . . . . .	35
Total horizontal-tail area, sq ft . . . . .	268
Horizontal-tail span, ft . . . . .	33
Horizontal-tail mean aerodynamic chord, in. . . . .	102.9
Horizontal-tail sweepback (25-percent-chord line), deg . . . . .	35
Airplane weight, lb . . . . .	100,000 to 120,000

TABLE II.- SUMMARY OF DEFLECTION AND TWIST MEASUREMENTS  
IN PULL-UPS AND IN ROUGH AIR

## (a) Deflection values

Wing station, in.	Target	Sensitivity factor, <u>Wing deflection</u> <u>Film deflection</u>	Pull-up factor, in./g	$\sigma_F$ , in.	$\frac{\sigma_F}{\sigma_R}$ (1)	$\sigma_e$ , in.
383	13	43.478	7.1	1.05	1.05	0.087
383	14	46.948	7.7	1.16	1.06	.094
517	11	34.965	13.1	2.00	1.08	.070
517	12	36.101	13.6	2.09	1.08	.072
681	9	46.296	21.7	3.39	1.10	.093
681	10	48.077	22.5	3.55	1.11	.096

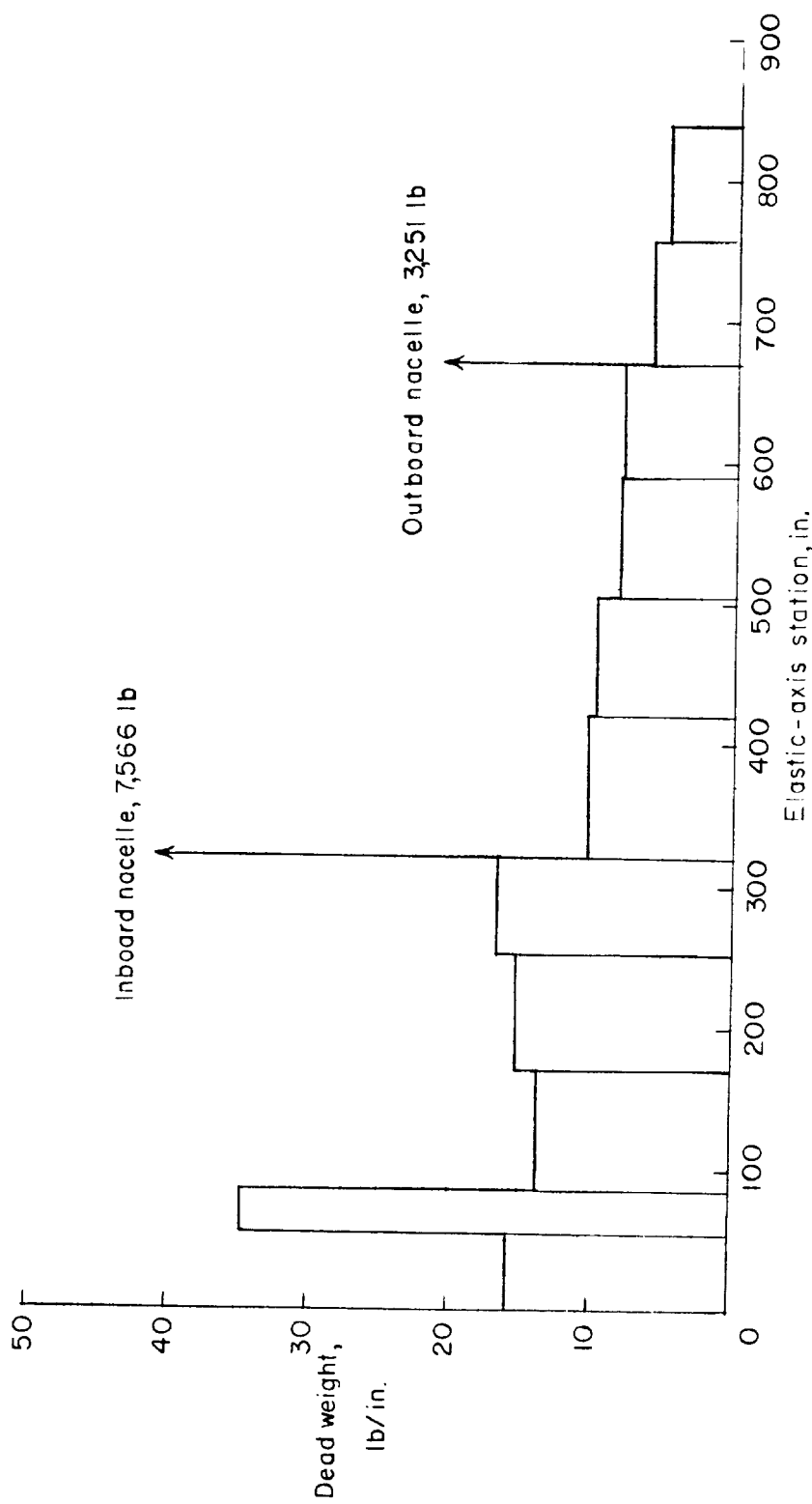
## (b) Twist values

Wing station, in.	$l_x$ , in.	Pull-up factor, radians/g	$\sigma_F$ , radians	$\frac{\sigma_F}{\sigma_R}$ (1)	$\sigma_e$ , radians
383	57.9	0.011	0.0025	1.59	0.0016
517	42.0	.013	.0051	2.78	.0017
681	54.5	.017	.0065	2.71	.0016

$$^1 \sigma_R = \sigma_{\bar{a}_n} = 0.14g \times \text{Pull-up factor.}$$

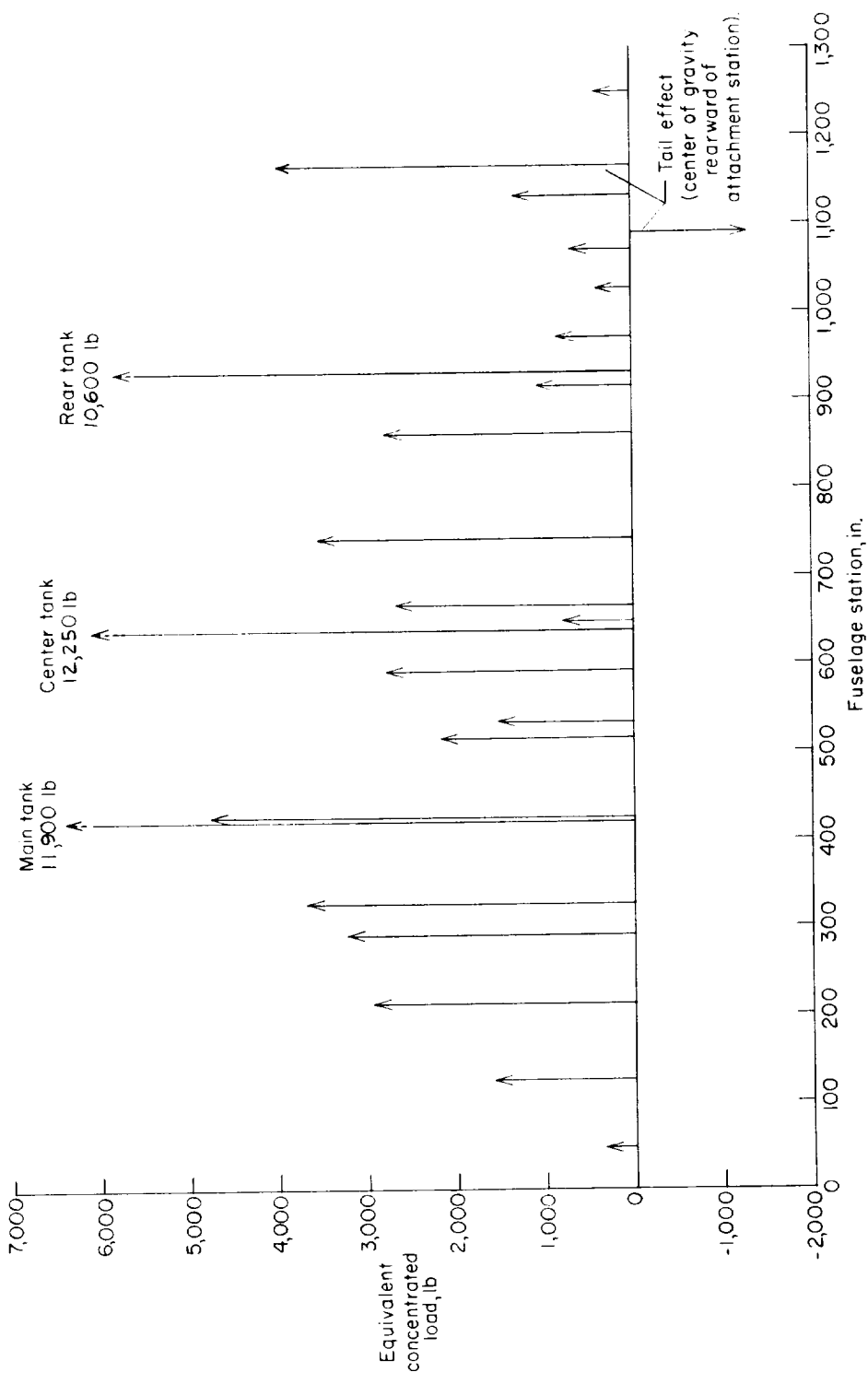


L-86692  
Figure 1.- Test airplane.



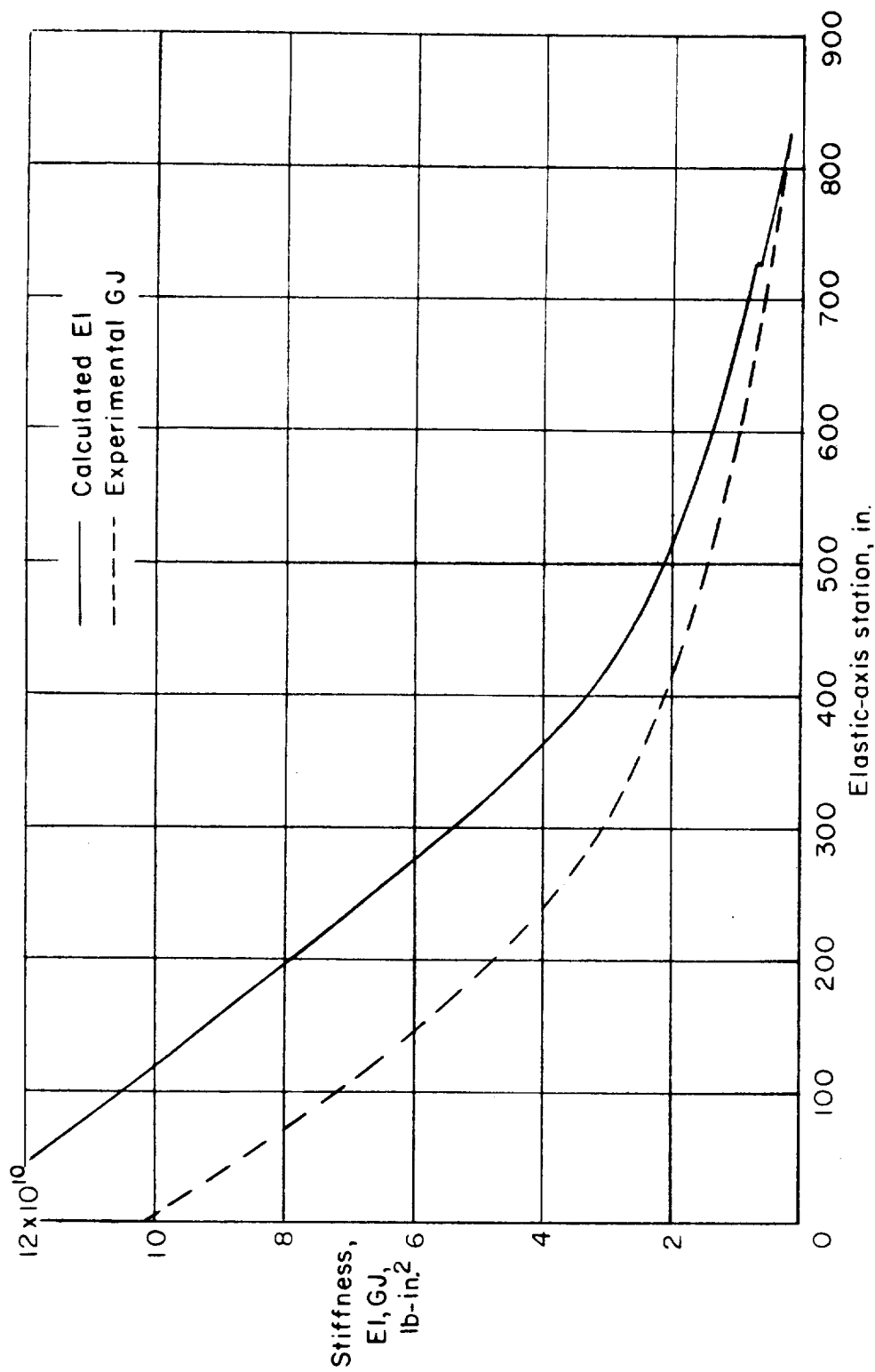
(a) Wing dead-weight distribution.

Figure 2.- Weight and stiffness distributions.



(b) Approximate weight distribution of fuselage including weight of pilots, instruments, and average fuel for gust test run.

Figure 2.- Continued.



(c) Bending and torsional-stiffness distribution of the wing.

Figure 2.- Concluded.

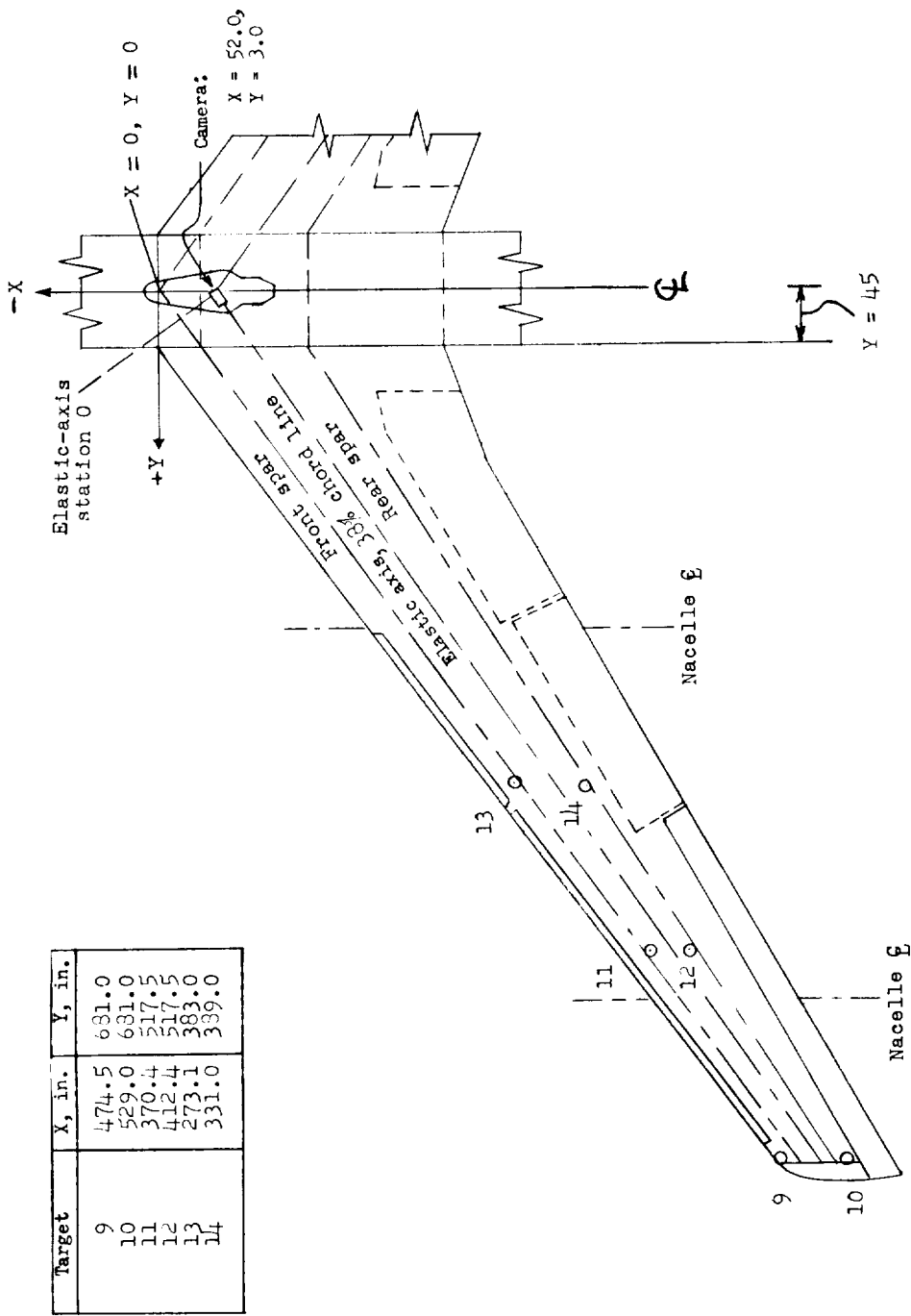
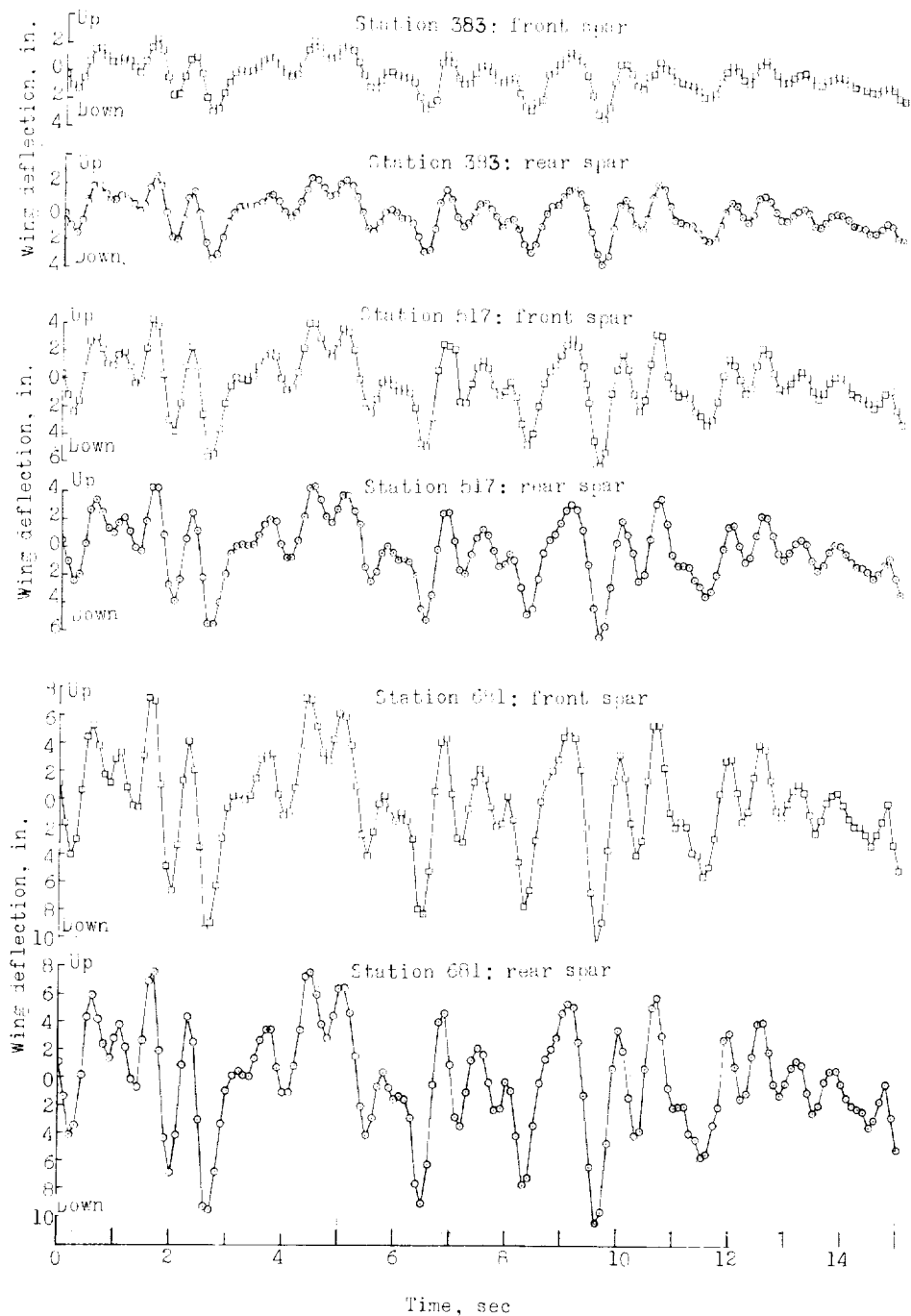
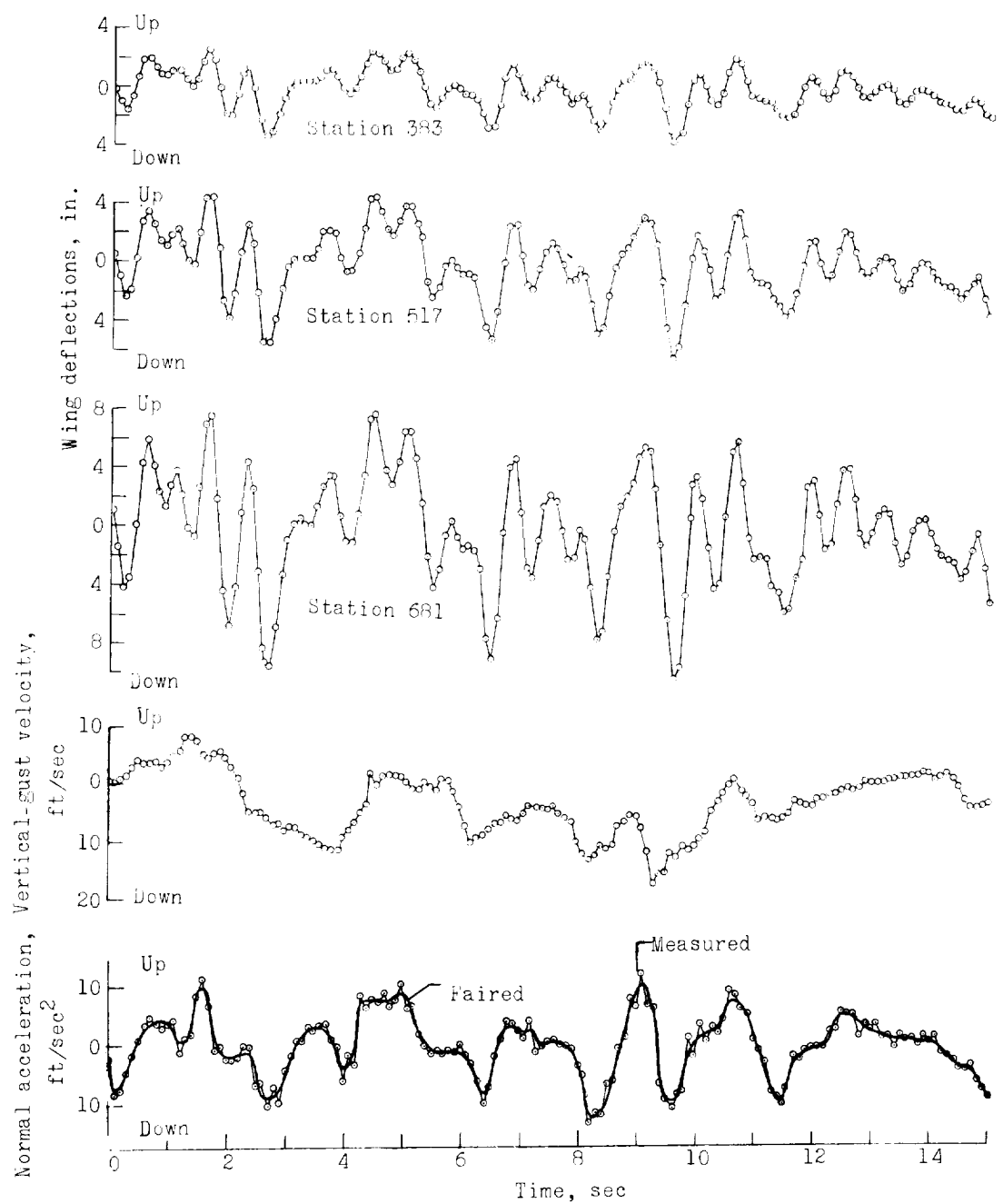


Figure 3.- Location of optograph camera and targets used during test.



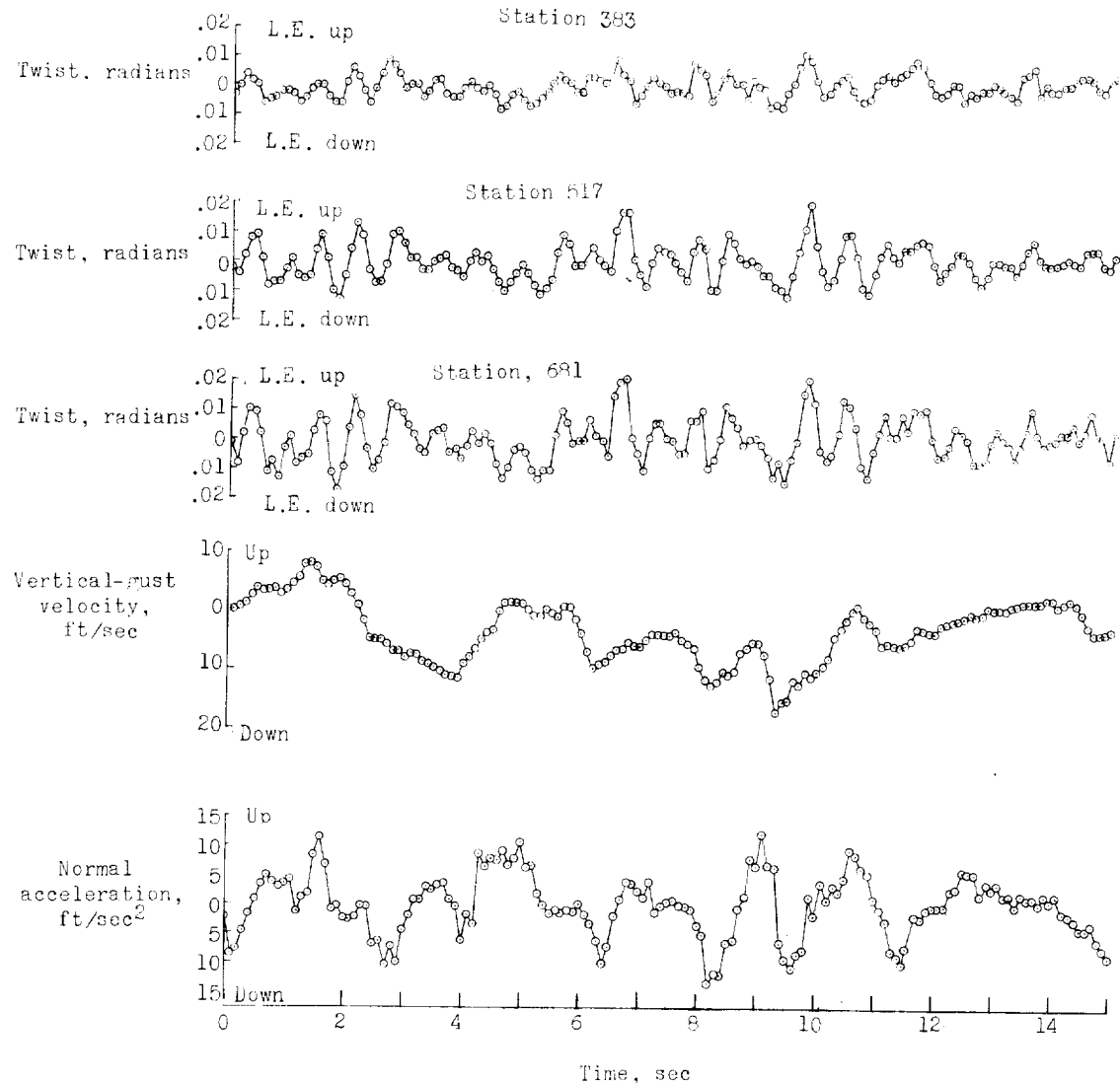
(a) Front- and rear-spar deflections.

Figure 4.- Sample time histories.



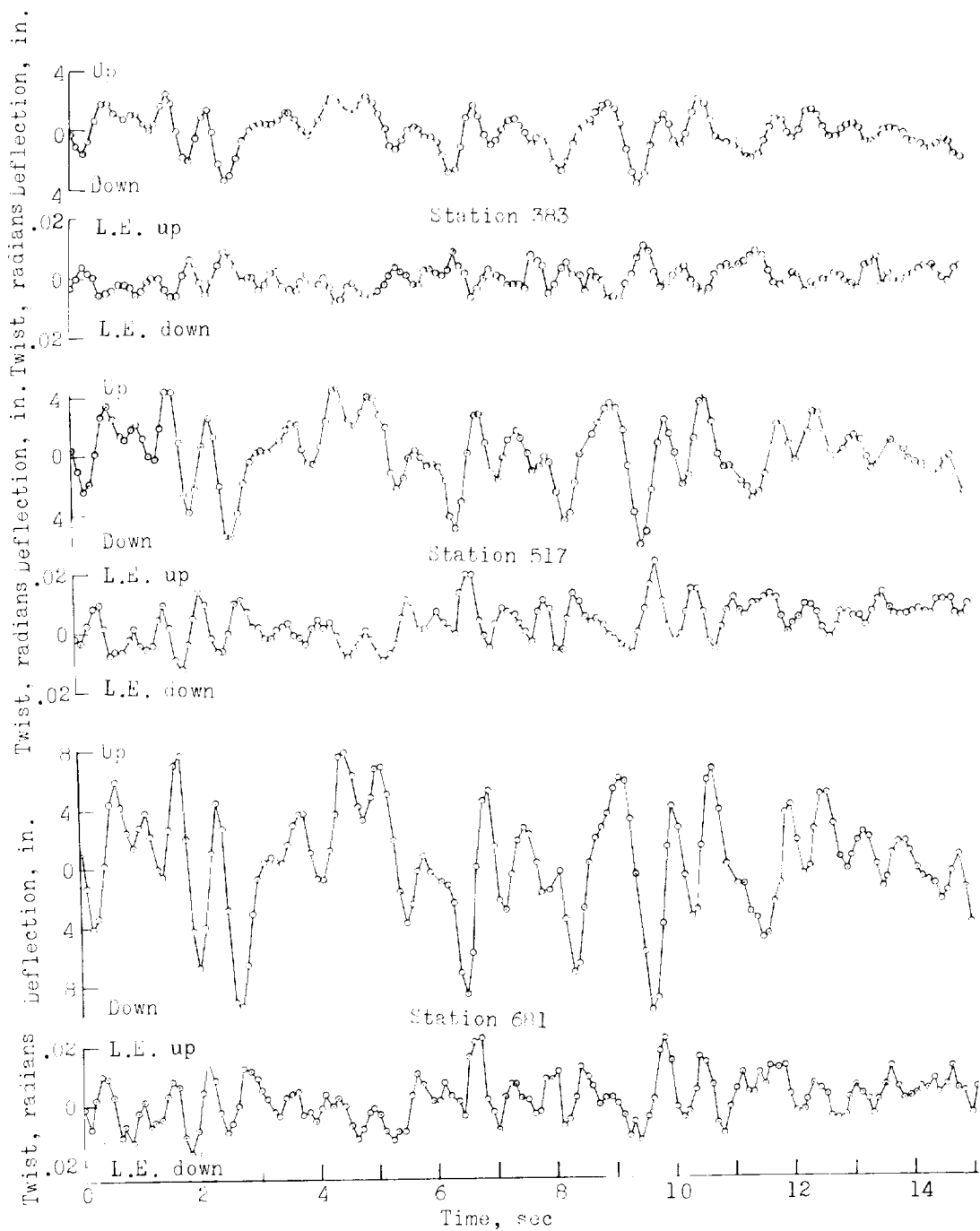
(b) Rear-spar deflections, vertical-gust velocity, and normal acceleration at center of gravity.

Figure 4.- Continued.



(c) Twist, vertical-gust velocity, and normal acceleration at center of gravity.

Figure 4.- Continued.



(d) Twist and rear-spar deflection at the three wing stations.

Figure 4-- Concluded.

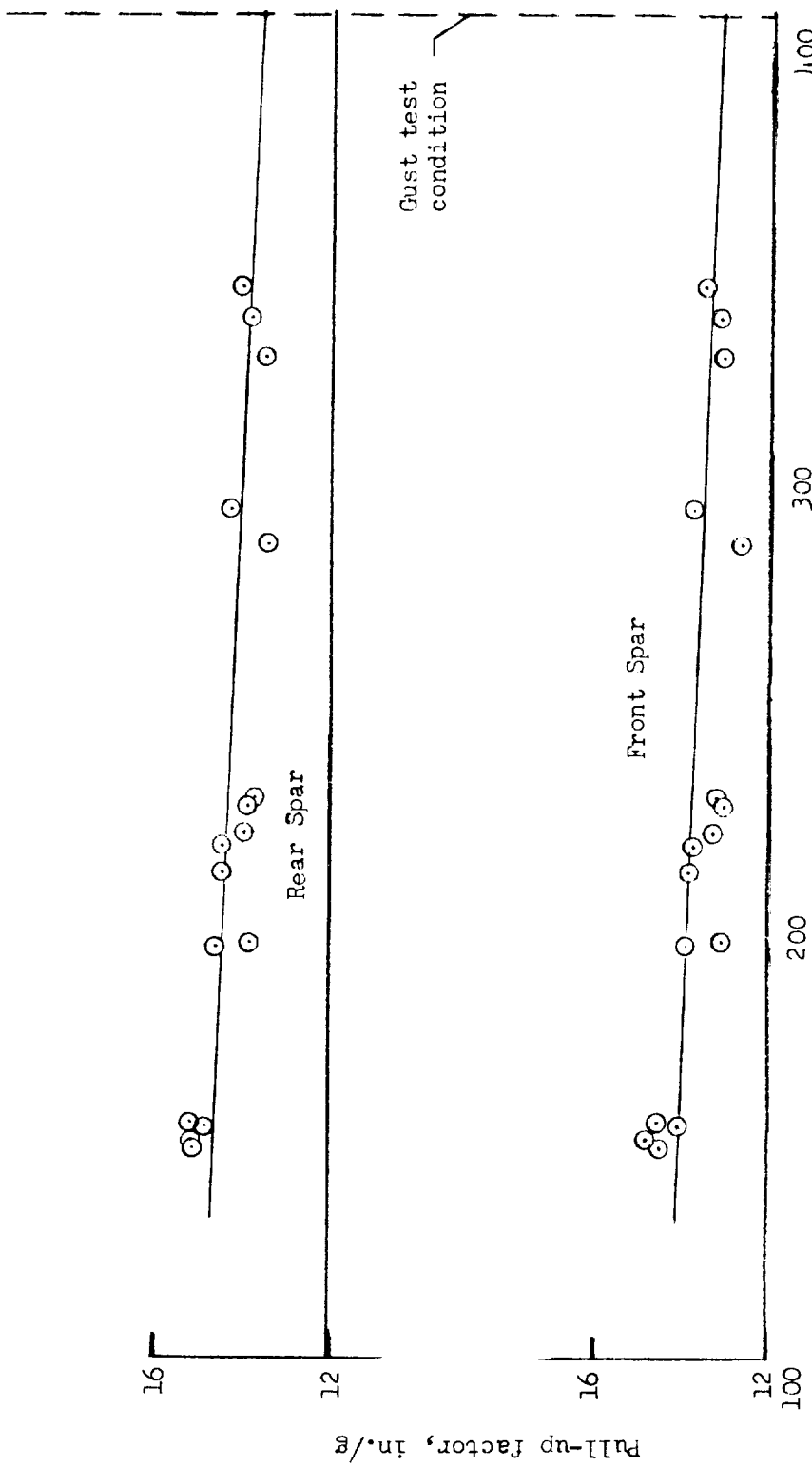
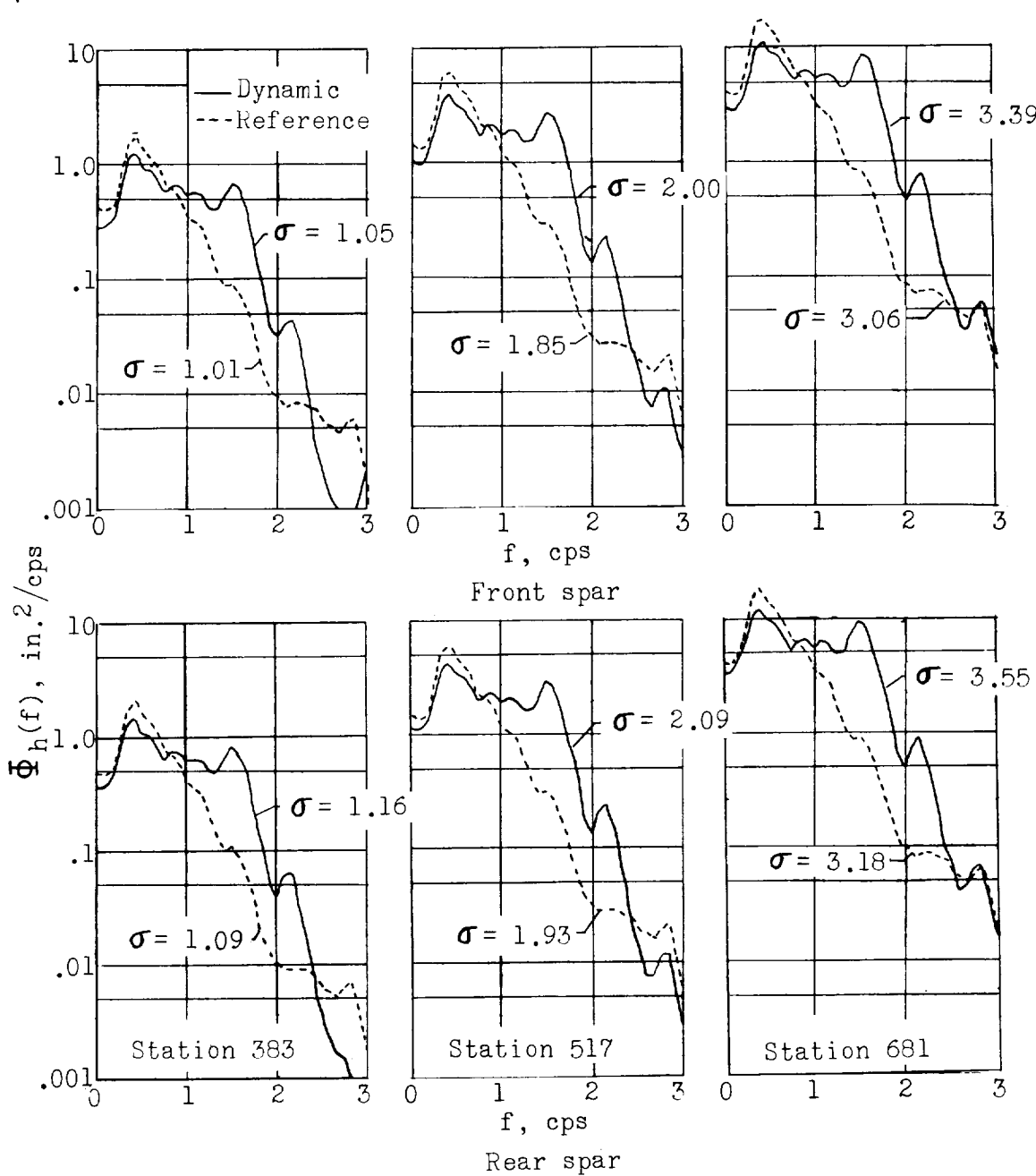
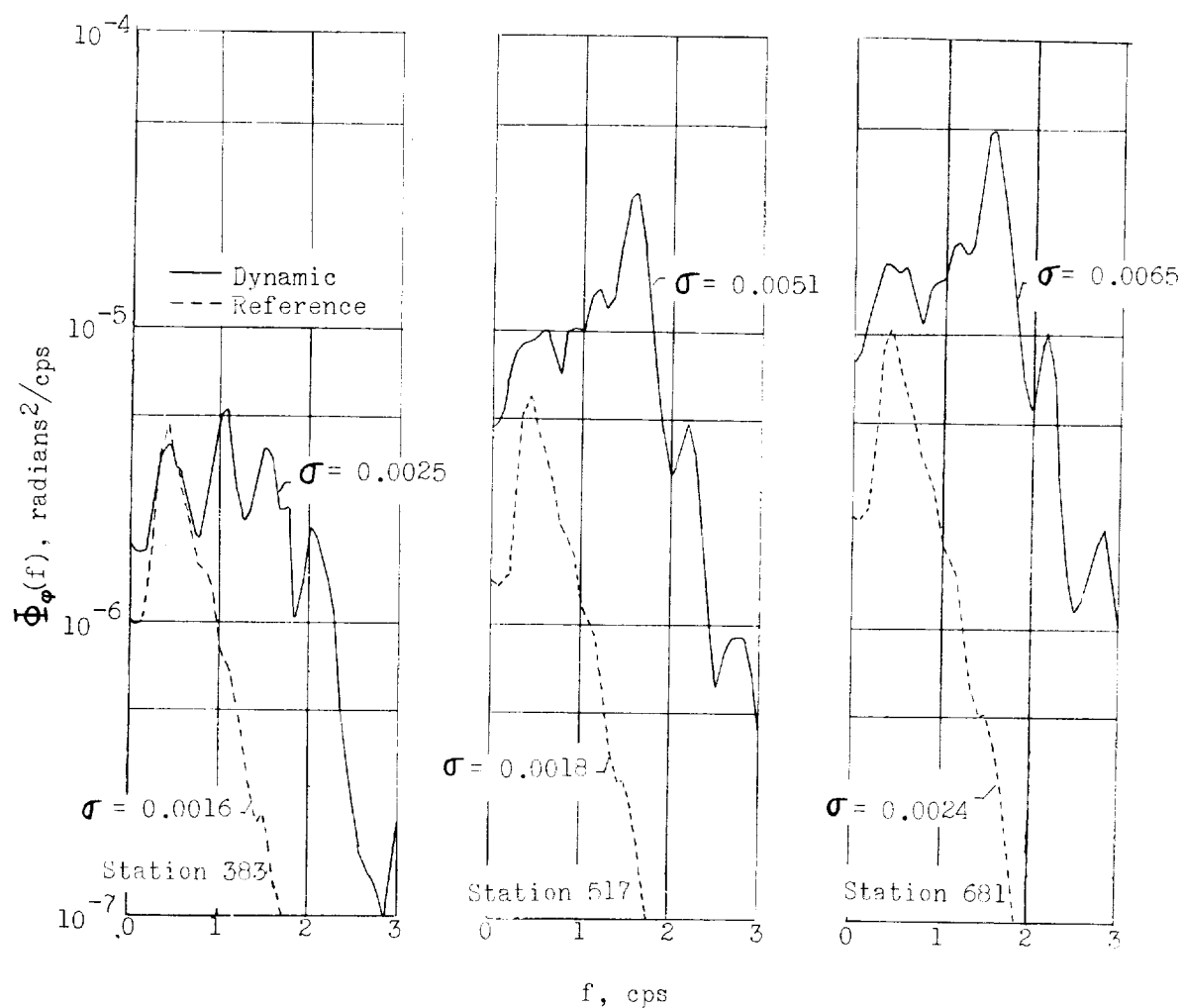


Figure 5.- Typical variation of pull-up factor with dynamic pressure. (Station 517.)



(a) Deflection spectra.

Figure 6.- Power spectra of deflection and twist.



(b) Twist spectra.

Figure 6.- Concluded.

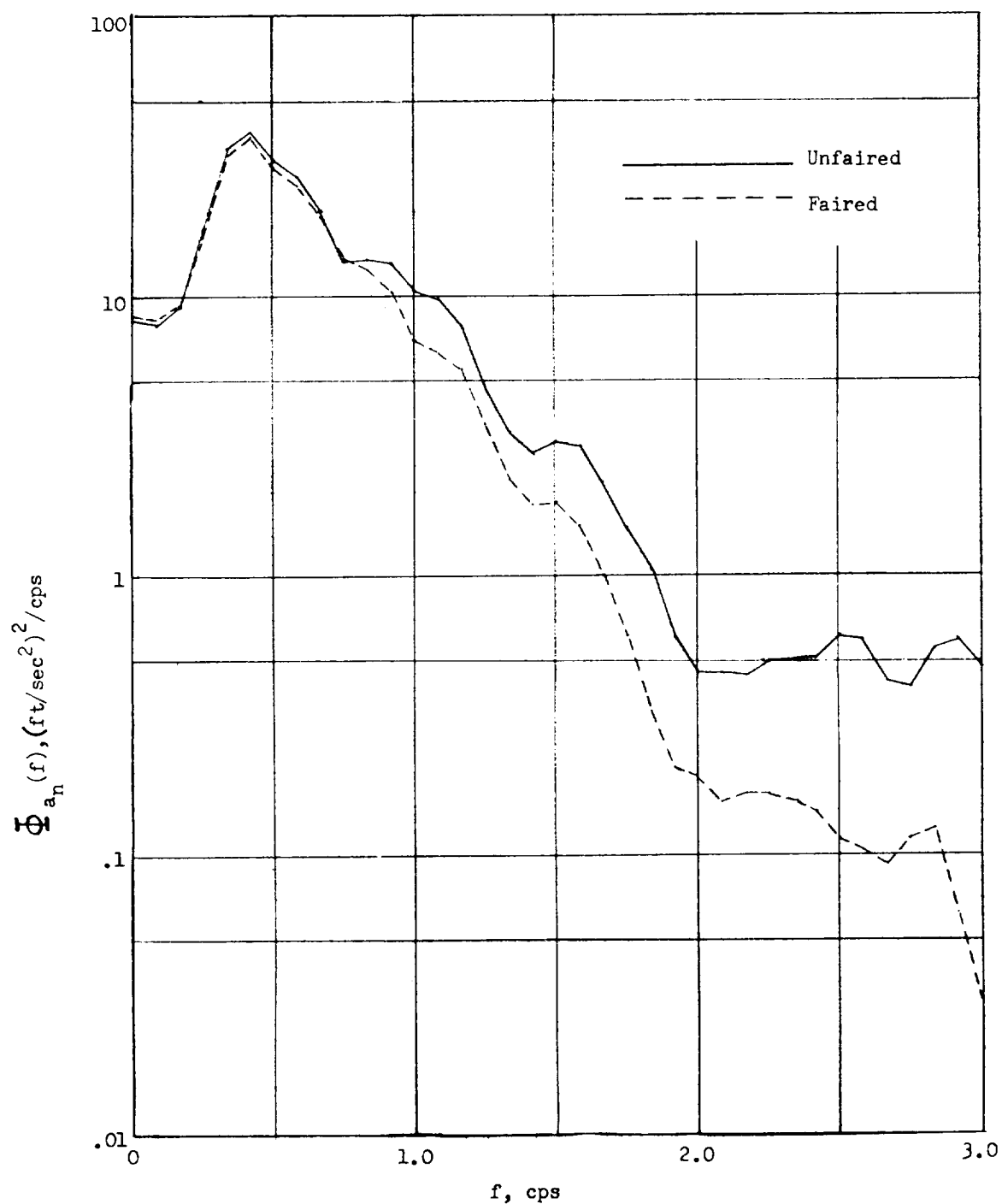


Figure 7.- Comparison of spectra of unfaired and faired center-of-gravity acceleration.

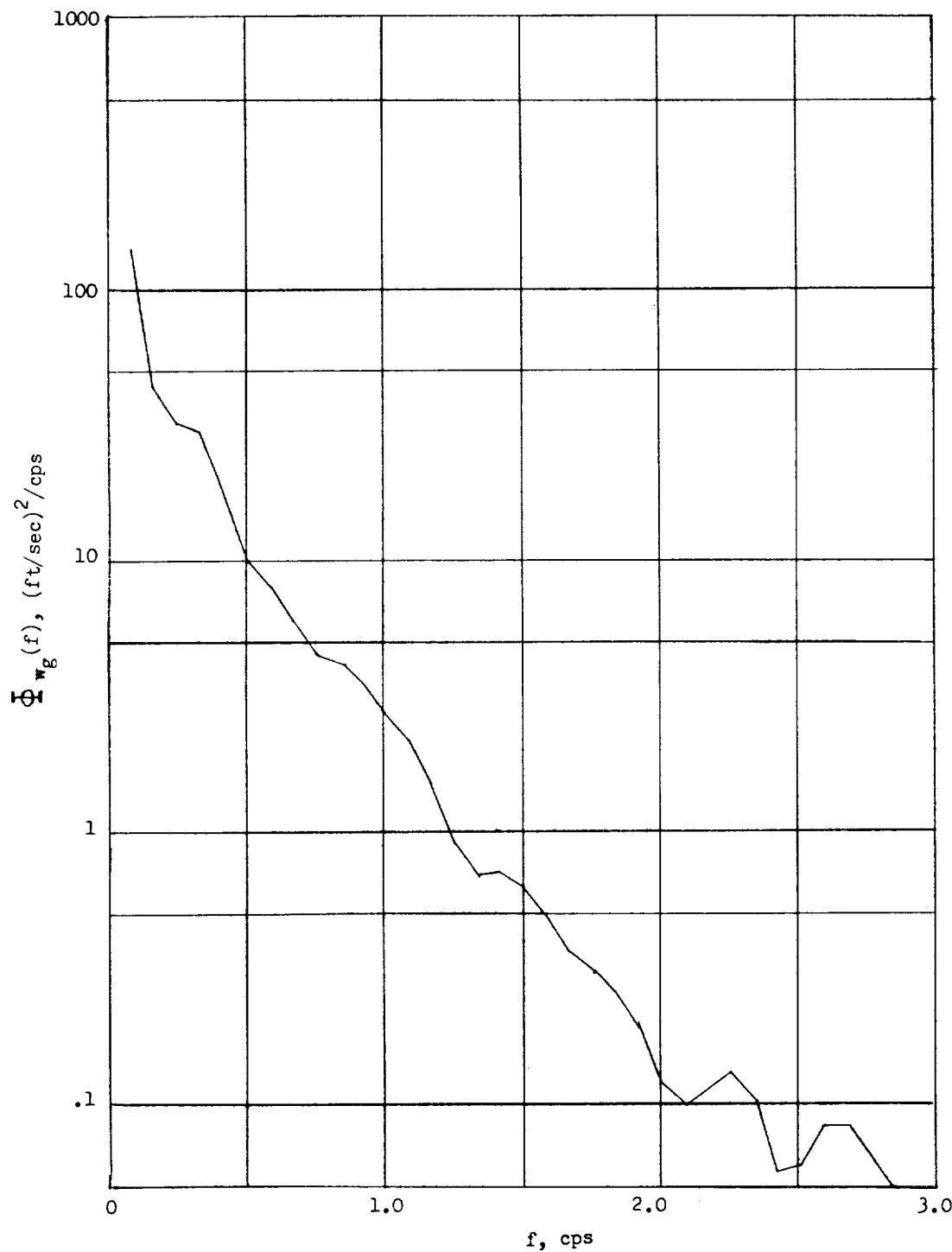
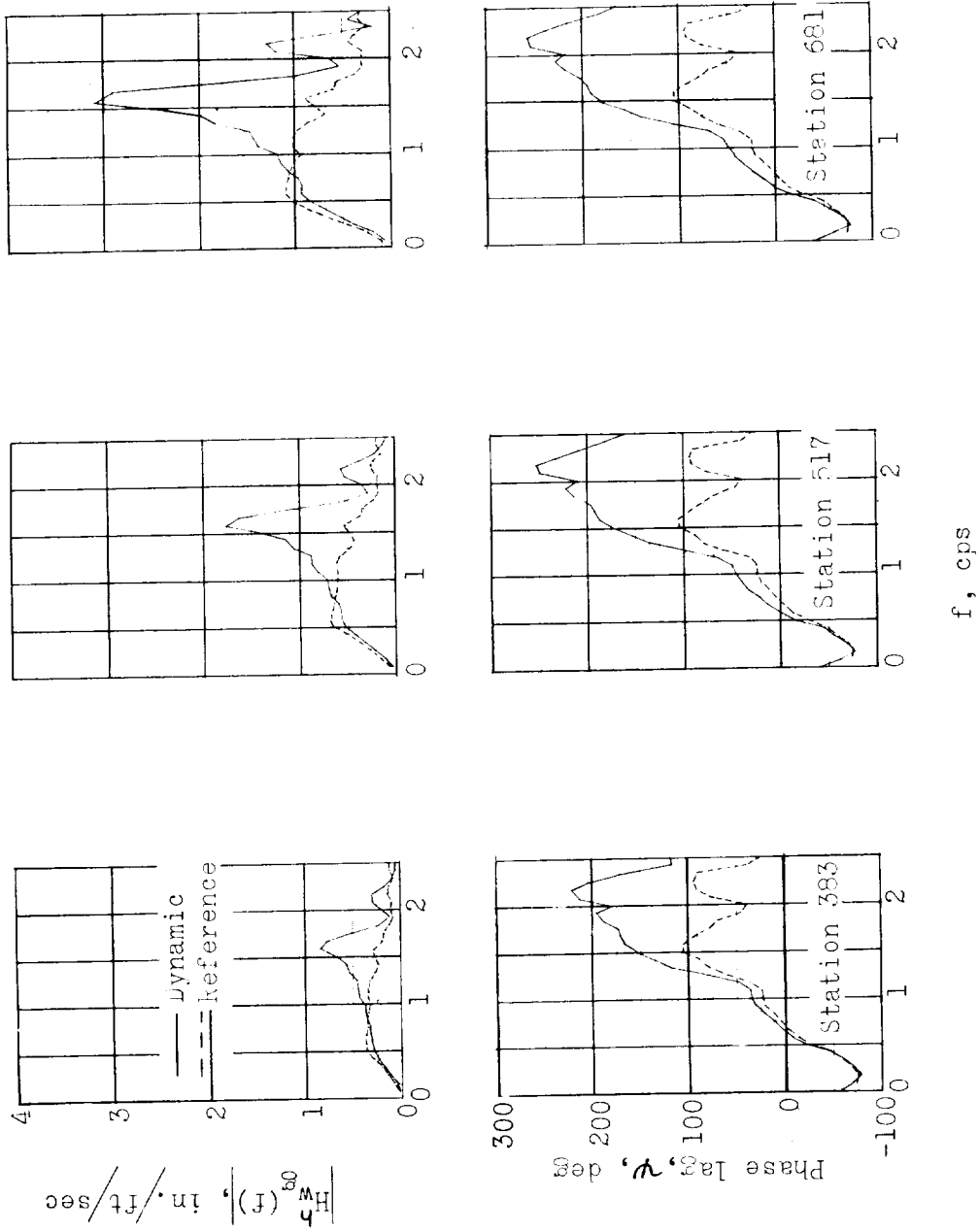
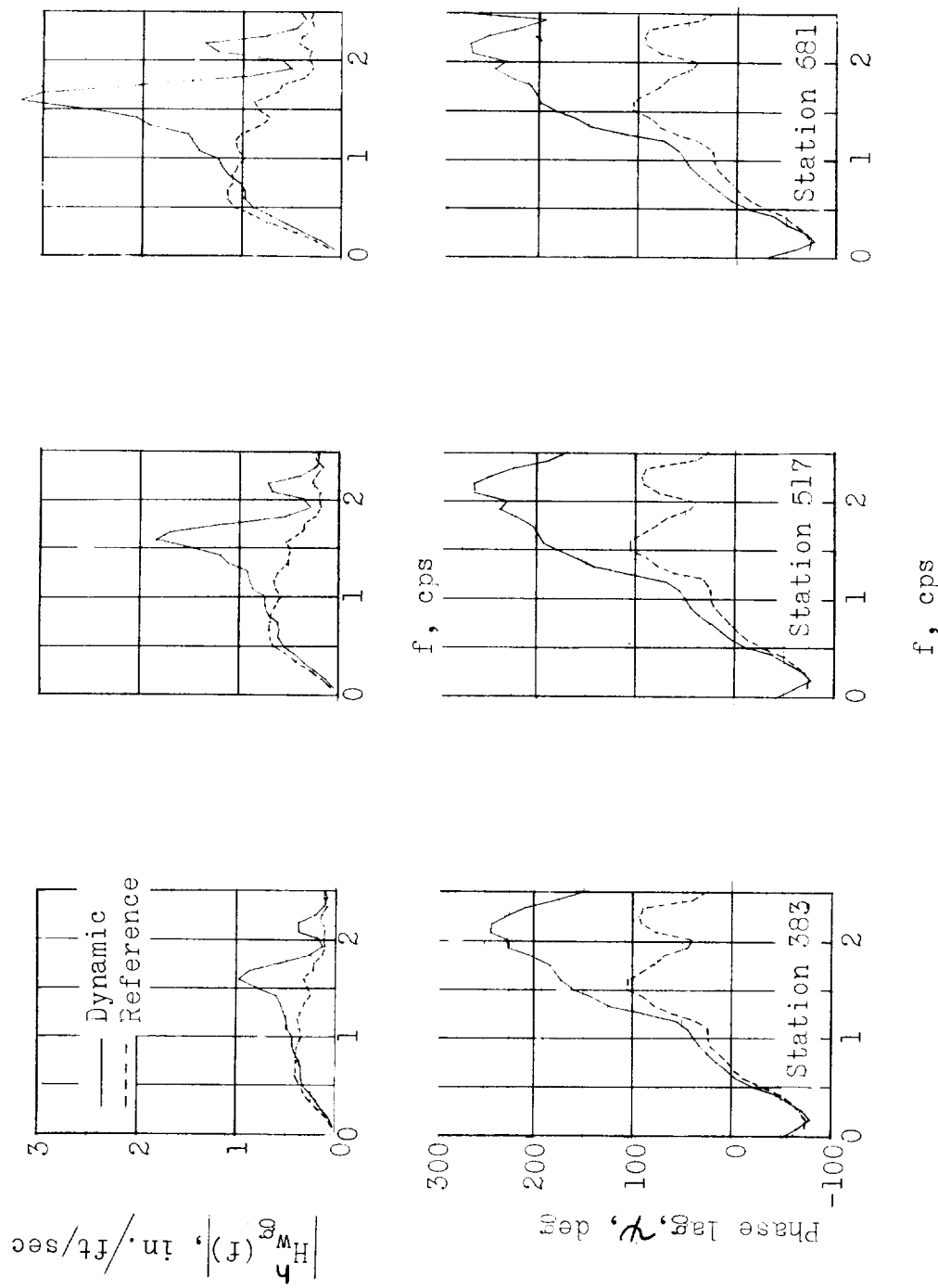


Figure 8.- Power spectrum of vertical-gust velocity.

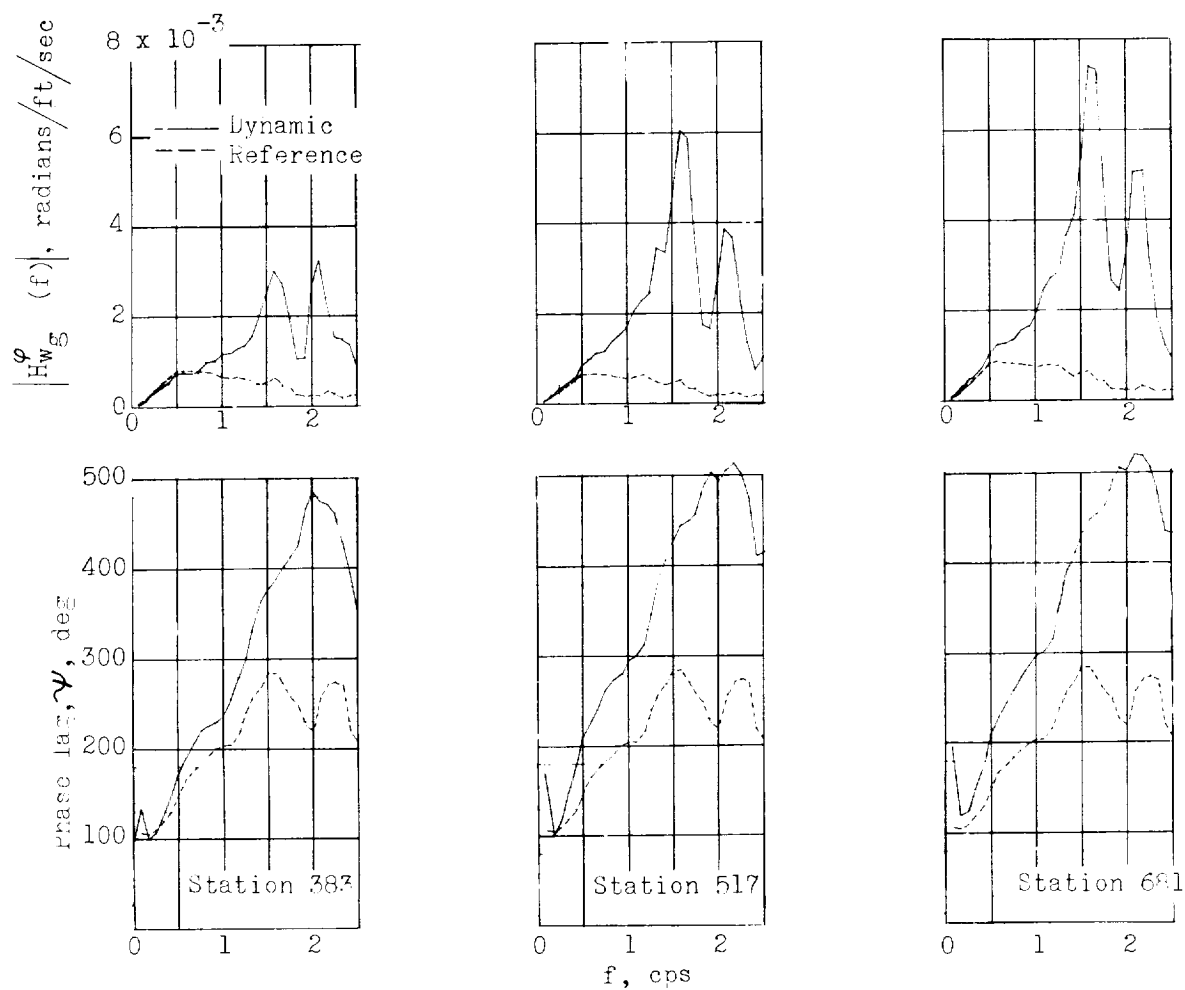


(a) Deflection of front spar.  
Figure 9.- Frequency responses of deflection and twist to vertical gusts.



(b) Deflection of rear spar.

Figure 9.- Continued.



(c) Twist.

Figure 9.- Concluded.

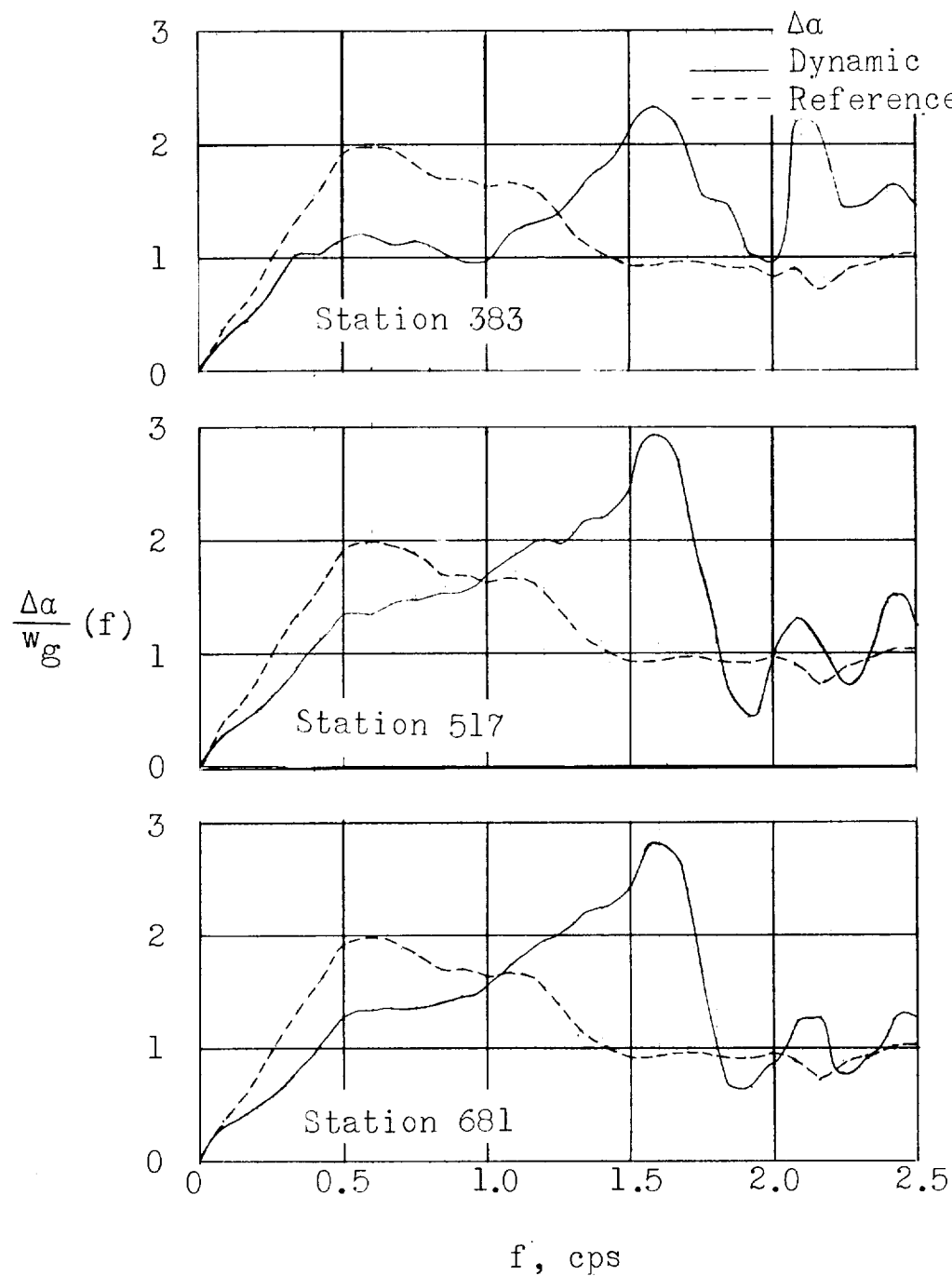
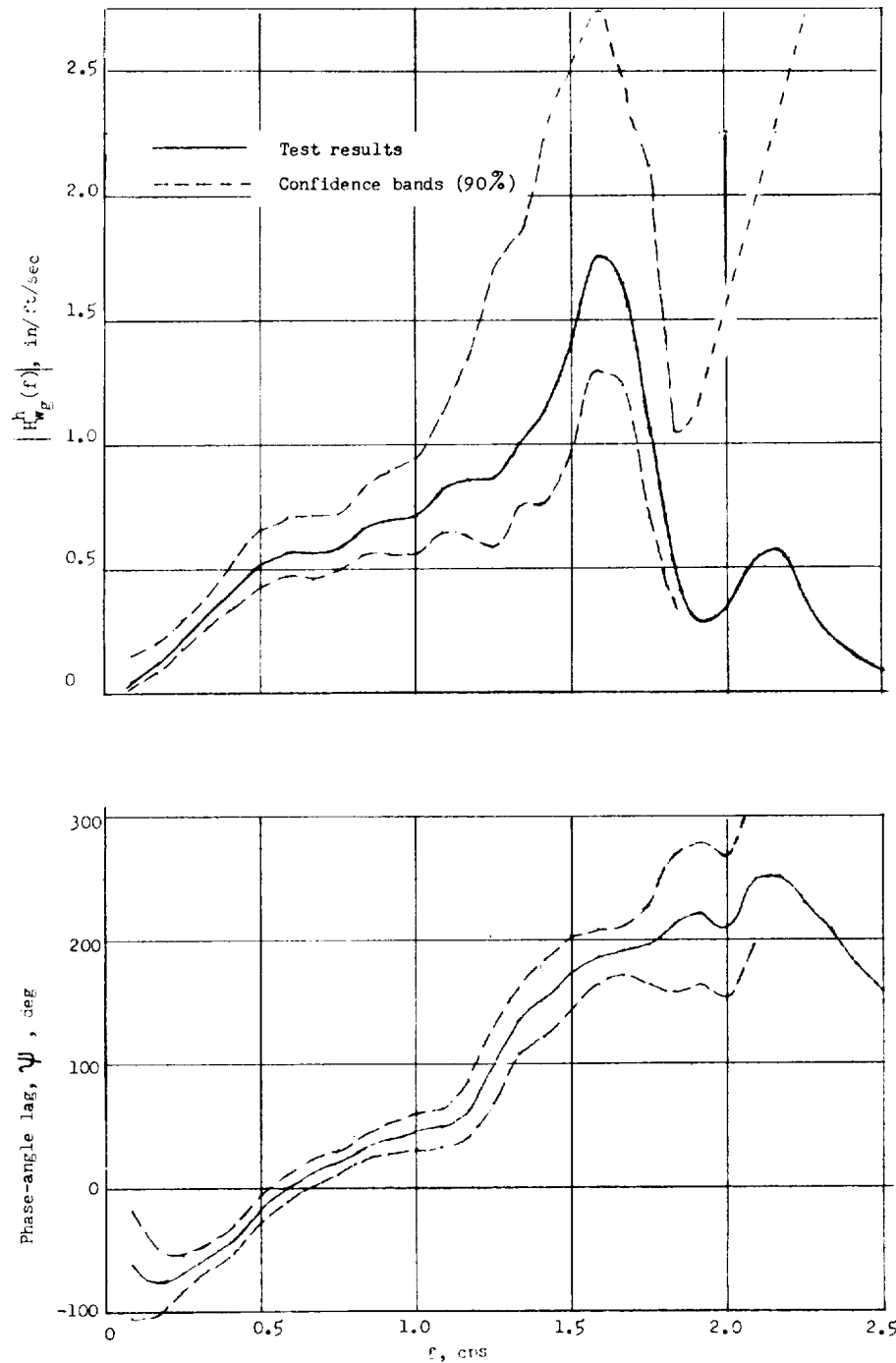
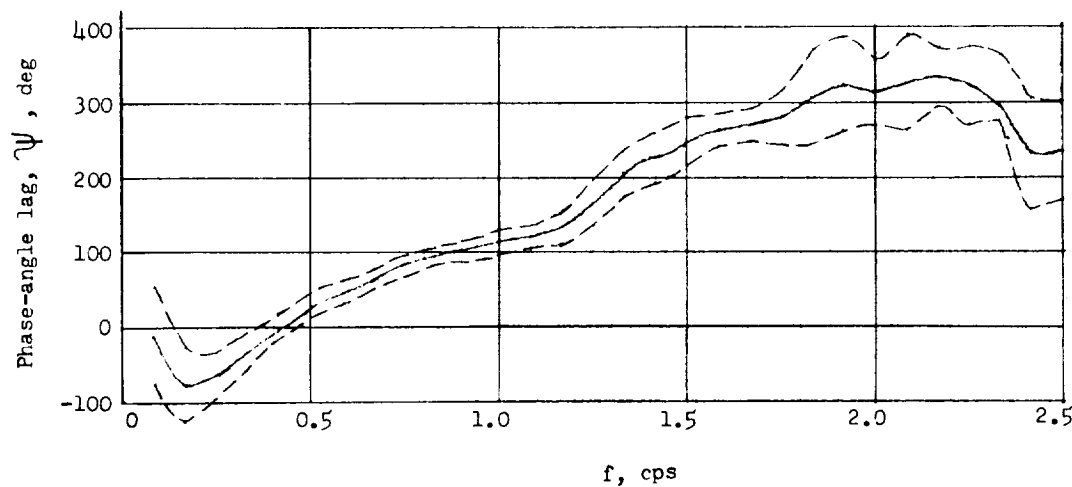
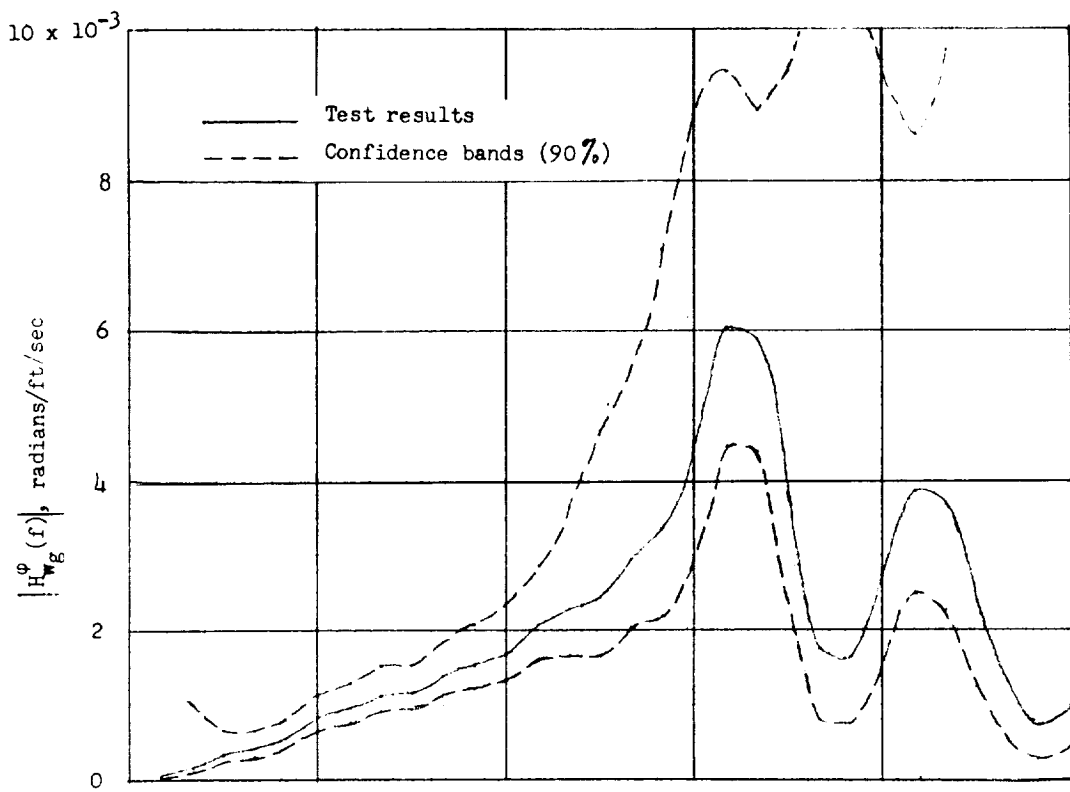


Figure 10.- Comparison of the ratio of local-angle-of-attack increment to the angle-of-attack increment due to a gust velocity of 1 fps for the dynamic and reference conditions.



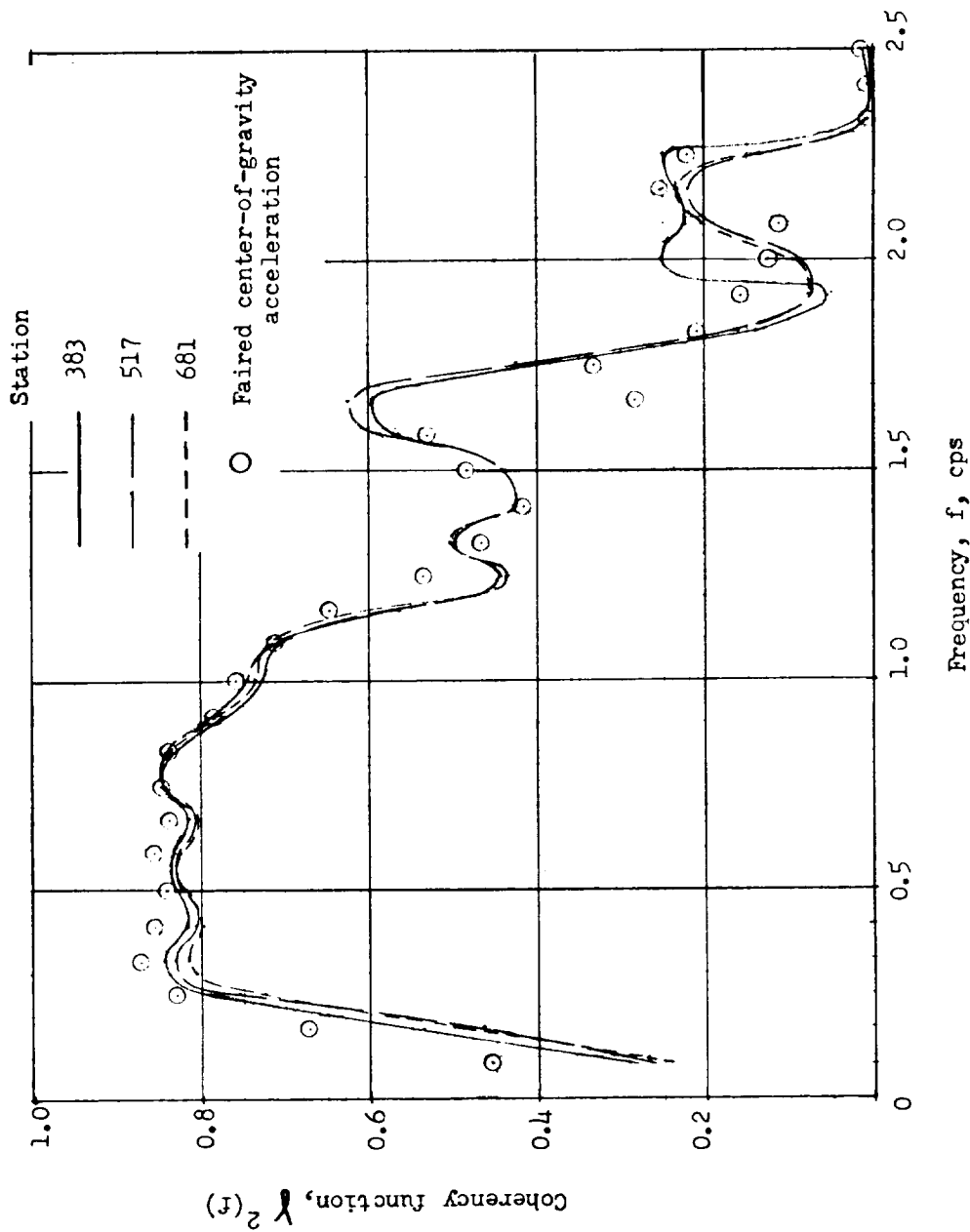
(a) Deflection of front spar at station 517.

Figure 11.- Confidence bands.



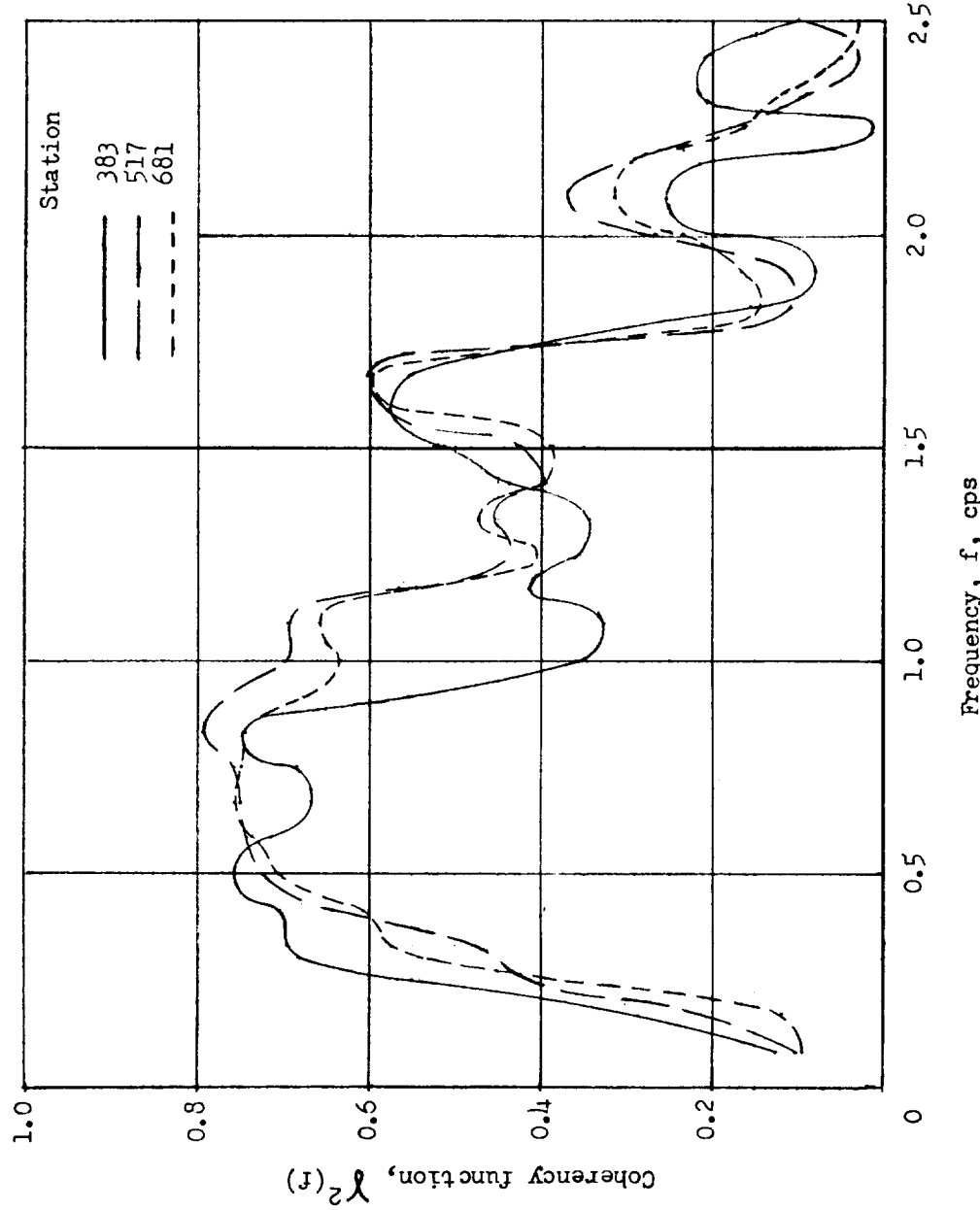
(b) Twist at station 517.

Figure 11.- Concluded.



(a) Front-spar deflections.

Figure 12.- Coherency functions.



(b) Twist.

Figure 12.- Concluded.

NASA MEMO 12-3-58L  
 National Aeronautics and Space Administration.  
**AN ANALYSIS OF FLIGHT-TEST MEASUREMENTS  
 OF THE WING STRUCTURAL DEFORMATIONS IN  
 ROUGH AIR OF A LARGE FLEXIBLE SWEPT-WING  
 AIRPLANE.** Harold N. Murrow. January 1959.  
 46p. diagrs., photo., tabs.  
 (NASA MEMORANDUM 12-3-58L)

From power spectral techniques, frequency-response functions are obtained for the deflection and twist responses at three spanwise locations to vertical gusts, and the results are compared with those obtained for a reference quasi-static airplane. The results obtained indicate that generally the deflections in rough air are amplified by a small amount, while the streamwise twists are amplified by factors of the order of 2.0. On a frequency basis, the maximum amplifications for both deflection and twist occur in the region of the first wing bending-mode frequency. An analysis of the effects of the deflection velocity

Copies obtainable from NASA, Washington (over)

NASA

1. Airplanes - Specific Types (1.7.1.2)  
 2. Loads, Gust - Wings (4.1.1.1.3)  
 3. Loads - Aeroelasticity (4.1.1.5)  
 4. Gusts, Atmospheric (6.1.2)

I. Murrow, Harold N.  
 II. NASA MEMO 12-3-58L

Copies obtainable from NASA, Washington (over)

NASA

NASA MEMO 12-3-58L  
 National Aeronautics and Space Administration.  
**AN ANALYSIS OF FLIGHT-TEST MEASUREMENTS  
 OF THE WING STRUCTURAL DEFORMATIONS IN  
 ROUGH AIR OF A LARGE FLEXIBLE SWEPT-WING  
 AIRPLANE.** Harold N. Murrow. January 1959.  
 46p. diagrs., photo., tabs.  
 (NASA MEMORANDUM 12-3-58L)

From power spectral techniques, frequency-response functions are obtained for the deflection and twist responses at three spanwise locations to vertical gusts, and the results are compared with those obtained for a reference quasi-static airplane. The results obtained indicate that generally the deflections in rough air are amplified by a small amount, while the streamwise twists are amplified by factors of the order of 2.0. On a frequency basis, the maximum amplifications for both deflection and twist occur in the region of the first wing bending-mode frequency. An analysis of the effects of the deflection velocity

Copies obtainable from NASA, Washington (over)

NASA

1. Airplanes - Specific Types (1.7.1.2)  
 2. Loads, Gust - Wings (4.1.1.1.3)  
 3. Loads - Aeroelasticity (4.1.1.5)  
 4. Gusts, Atmospheric (6.1.2)

I. Murrow, Harold N.  
 II. NASA MEMO 12-3-58L

Copies obtainable from NASA, Washington (over)

NASA

NASA MEMO 12-3-58L  
 National Aeronautics and Space Administration.  
**AN ANALYSIS OF FLIGHT-TEST MEASUREMENTS  
 OF THE WING STRUCTURAL DEFORMATIONS IN  
 ROUGH AIR OF A LARGE FLEXIBLE SWEPT-WING  
 AIRPLANE.** Harold N. Murrow. January 1959.  
 46p. diagrs., photo., tabs.  
 (NASA MEMORANDUM 12-3-58L)

From power spectral techniques, frequency-response functions are obtained for the deflection and twist responses at three spanwise locations to vertical gusts, and the results are compared with those obtained for a reference quasi-static airplane. The results obtained indicate that generally the deflections in rough air are amplified by a small amount, while the streamwise twists are amplified by factors of the order of 2.0. On a frequency basis, the maximum amplifications for both deflection and twist occur in the region of the first wing bending-mode frequency. An analysis of the effects of the deflection velocity

Copies obtainable from NASA, Washington (over)

NASA

1. Airplanes - Specific Types (1.7.1.2)  
 2. Loads, Gust - Wings (4.1.1.1.3)  
 3. Loads - Aeroelasticity (4.1.1.5)  
 4. Gusts, Atmospheric (6.1.2)

I. Murrow, Harold N.  
 II. NASA MEMO 12-3-58L

Copies obtainable from NASA, Washington (over)

NASA

NASA MEMO 12-3-58L

and twisting motions on the local angles of attack is  
also presented.

NASA MEMO 12-3-58L

and twisting motions on the local angles of attack is  
also presented.

Copies obtainable from NASA, Washington

NASA MEMO 12-3-58L

and twisting motions on the local angles of attack is  
also presented.

NASA

Copies obtainable from NASA, Washington

NASA MEMO 12-3-58L

and twisting motions on the local angles of attack is  
also presented.

NASA

Copies obtainable from NASA, Washington

NASA

Copies obtainable from NASA, Washington